Influence of Camouflage on the ATR Performance for Highly Resolved ISAR-Images of Relocatable Targets

Timo Kempf, Markus Peichl, Stephan Dill, Helmut Süß

DLR (German Aerospace Center), Microwave and Radar Institute,
P.O.-Box 11 16, 82230 Wessling, Germany

Abstract:

By means of data from highly resolved tower-turntable ISAR measurements this paper investigates the influence of camouflage on the ATR performance. The recognition process is based on a template matching method. The two-dimensional templates are generated by extracting the most robust scatterers from the RCS image.

Keywords: ISAR, high resolution, ATR, camouflage, ROC curves.

1. Introduction

Global and reliable reconnaissance using remote sensing techniques requires weather and daytime independent detection, recognition, and identification of interesting objects. Thus a spaceborne high resolution (HR) synthetic aperture radar (SAR) system in a spotlight mode can be an appropriate instrument. On this basis we undertook X-band I(nverse)SAR-measurements on a tower-turntable arrangement to get highly resolved two-dimensional signatures of military and civilian relocatable targets for adequately steep depression angles. Our work is focused on military vehicles, and we use civilian vehicles as confusers.

Since typical military vehicles consist of several ideally behaving scattering centers which show some robustness to aspect variations, we established a recognition method based on the extraction of these point scatterers. Furthermore, with a demanded declaration time that is sufficiently long, we have the freedom to perform classification via a computationally intensive template matching process. Moreover this method ensures a sufficient inner class robustness, while simultaneously yielding efficient inter class separability.

In [1] we gave an overview of the performance of the mentioned ATR method using the tower-turntable database, which includes several thousand templates. The focus was set on the investigation of the robustness by using different articulations of the targets in training and testing. The results showed a good robustness to different realizations and poses of one target type but a high sensitivity to the sensor-target geometry.

In this paper we want to investigate the influence of different camouflage and deception methods on the ATR performance. Therefore we look into more details of the data bases we established in the mentioned measurement campaigns. More precisely, we look on cases of natural camouflage, camouflage by radar nets, confusing by adding scattering centers and finally on the result of a decoy. For the evaluation of the ATR results, the commonly used receiver operating characteristic (ROC) curves are computed.

2. ISAR set-up and image processing

In [2] we already introduced a kind of fingerprint analysis as a situation-optimized tool for reliable target recognition. The development and investigation of our method is based on ISAR measurements in X band. They had been realized on a suitable tower-turntable arrangement as shown in fig. 1 on military vehicles for different steep depression angles.

These data have been used to develop a processing scheme that delivers a filtered and digitized radar image of those target scatteres, which behave almost like ideal point scatterers and which are robust to aspect angle variations. The filtering includes a sidelobe suppression by maintaining the original resolution and a phase analysis for the extraction of the most robust scatterers.

In a practical use of a military reconnaissance operation such digitized images of an actual scene of interest can be compared successively to similarly processed image templates of a database. In principle, a type specific classifier correlates the current digitized

Kempf, T.; Peichl, M.; Dill, S.; Süß, H. (2005) Influence of Camouflage on the ATR Performance for Highly Resolved ISAR-Images of Relocatable Targets. In *MMW Advanced Target Recognition and Identification Experiment* (pp. 2-1 – 2-12). Meeting Proceedings RTO-MP-SET-096, Paper 2. Neuilly-sur-Seine, France: RTO. Available from: http://www.rto.nato.int/abstracts.asp.

Report Documentation Page

Form Approved
OMB No. 0704-0188

1. REPORT DATE	2. REPORT TYPE	3. DATES COVERED
01 MAY 2005	**N/A**	**-**

4. TITLE AND SUBTITLE
Influence of Camouflage on the ATR Performance forHighly Resolved ISAR-Images of Relocatable Targets

5a. CONTRACT NUMBER

5b. GRANT NUMBER

5c. PROGRAM ELEMENT NUMBER

6. AUTHOR(S)

5d. PROJECT NUMBER

5e. TASK NUMBER

5f. WORK UNIT NUMBER

7. PERFORMING ORGANIZATION NAME(S) AND ADDRESS(ES)
DLR (German Aerospace Center), Microwave and Radar Institute, P.O.-Box 11 16, 82230 Wessling, Germany

8. PERFORMING ORGANIZATION REPORT NUMBER

9. SPONSORING/MONITORING AGENCY NAME(S) AND ADDRESS(ES)

10. SPONSOR/MONITOR'S ACRONYM(S)

11. SPONSOR/MONITOR'S REPORT NUMBER(S)

12. DISTRIBUTION/AVAILABILITY STATEMENT
Approved for public release, distribution unlimited

13. SUPPLEMENTARY NOTES
See also ADM202152., The original document contains color images.

14. ABSTRACT

15. SUBJECT TERMS

16. SECURITY CLASSIFICATION OF:			17. LIMITATION OF ABSTRACT	18. NUMBER OF PAGES	19a. NAME OF RESPONSIBLE PERSON
a. REPORT	b. ABSTRACT	c. THIS PAGE			
unclassified	**unclassified**	**unclassified**	**UU**	**32**	

Standard Form 298 (Rev. 8-98)
Prescribed by ANSI Std Z39-18

test image with each training image, delivering the highest of the generated correlation values. In the following this value is also used as 'discrimination value'.

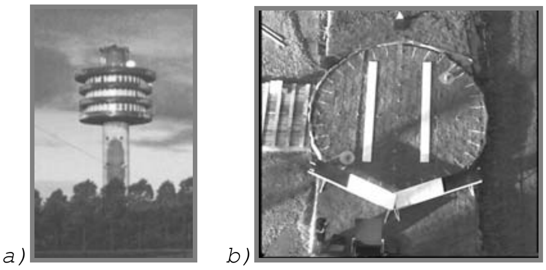

Figure 1: Tower-turntable setup for ISAR measurements, a) four platforms on the tower allow different incidence angles, b) the tilting turntable was covered with soil and grass for a realistic ground, having 9m in diameter and a payload up to 100t.

Our first results indicated that this kind of fingerprint analysis can deliver reliable recognition results with a feasible amount of computational effort.

The target list of our last campaign included military and civilian vehicles, whereas the intention of the ATR system design is focused on the military targets and the civilian vehicles are mainly used as confusers. For the camouflage investigations we extract the results of classifiers for three different target types. For our purposes here, it is sufficient to name these three types 'A', 'B', and 'C'. The corresponding classifiers are named 'C_A', 'C_B', and 'C_C'.

3. ATR tests on scenes with camouflaged targets

Following, we present results for camouflage on military vehicles by covering with branches of birch trees, covering with a radar net, or by a kind of confusing by covering the surrounding ground of the target with metal plates. Additionally, we show the result of a decoy. Each data set consists of 72 images for a 360° aspect range.

For illustration we show photographs and radar images of the scene for the eight cardinal and semicardinal directions. The first row of radar images shows unfiltered, non-weighted signatures (the highly resolved radar cross section RCS) of the test scene in the photograph. The second row includes the filtered and digitized radar images, which are used as template for the recognition process. The third radar image row shows the relevant training data of the uncovered target. The fourth row includes the unfiltered images of the original scenes.

Except for the camouflage, the scene of the test case is not changed compared to the training case. Small variations occur in the azimuth sampling, caused by a slightly inhomogenous rotation of the turntable. This means, as we find here an almost ideal replication of the training situation, variations in the recognition performance can be assigned directly to the current kind and way of camouflage.

3.1 Camouflage by covering

In this section we discuss the results of camouflage by covering either with natural materials like birch branches or with an artificial radar net. First, we investigate the effect of natural camouflage on the ATR performance. Therefore a battle tank and a smaller armoured track vehicle were illuminated. The camouflage is mounted in a way as it is suppossed to be done in the field. Primarily, this means a covering of the upper structures of the vehicle.

3.1.1 Natural camouflage

A separate test on the birch branches used in the following revealed an attenuation in our radar system of about 10dB. In fig. 2 we see the example of a battle tank, here target 'A', covered with branches of a birch tree. The digitized images of test and training, so the images of the target with and without natural camouflage show differences. Whether these differences have an impact on the recognition performance a more detailed analysis has to show.

Therefore the discrimination values of the classifier trained on this type of target (C_A) are plotted in fig. 3. A discrimination value d_A=1.0 would signify perfect identity of test and training template.

Fig. 3a) shows the discrimination plot of classifier C_A for 6 scenes. The second scene is the one presented in fig. 2, the other scenes contain confusers or other targets. For an ideal recognition, all the discrimination values of C_A in scene 2 should be above the values of C_A in the other scenes. For better comparison we establish a reference line (dashed) representing a threshold, for which 99 percent of the discrimination values in the other target scenes or confuser scenes are below.

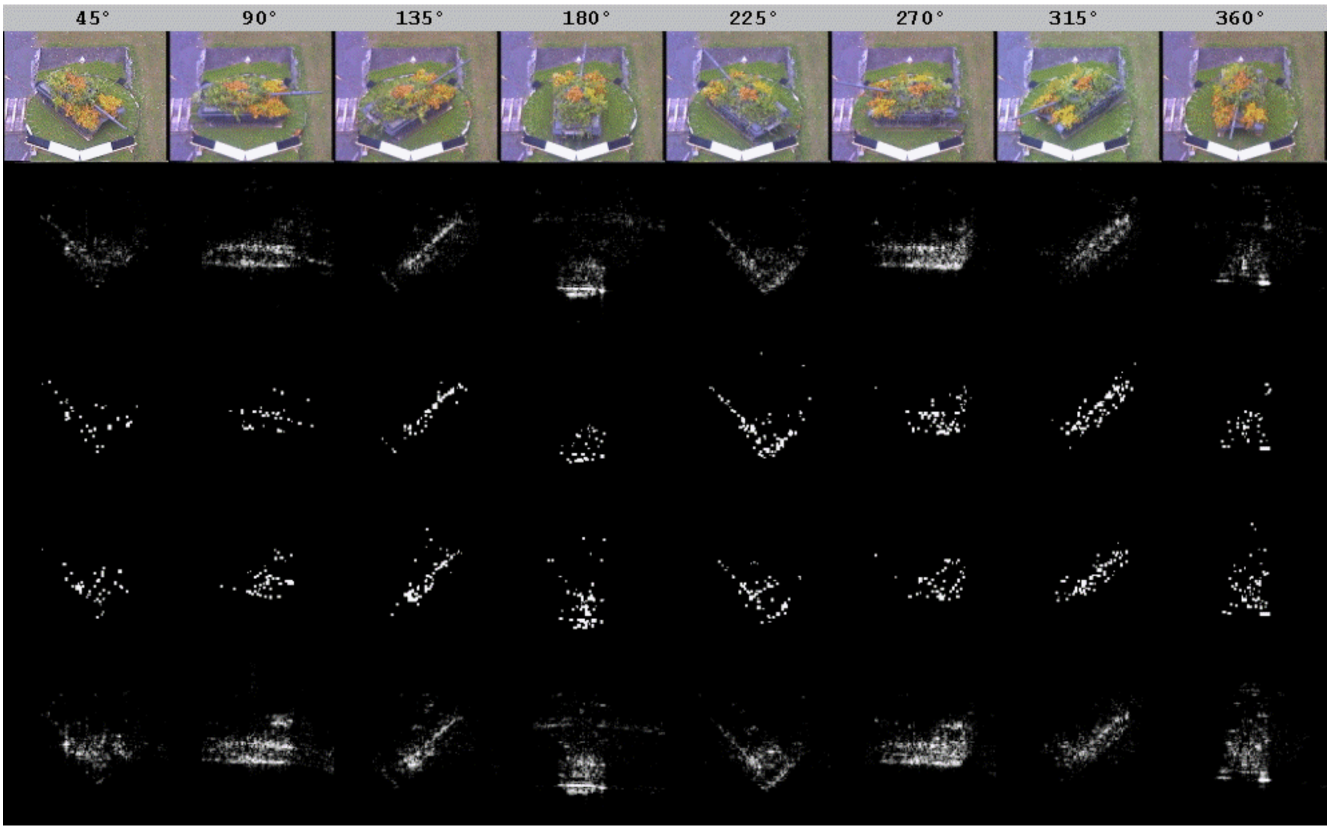

Figure 2: Images of target 'A', a battle tank covered with birch branches for positions 45°, 90°, 135°, 180°, 225°, 270°, 315° and 360°. First row: photograph (test scene), second row: RCS image of the test scene, third row: ATR relevant digitized image of the test scene, lower second row: digitized image of the training scene (uncovered target), lower row: RCS image of the training scene (uncovered target).

The result of scene 2 is plotted in higher resolution for clarity in fig. 3b, showing that in some cases the threshold is not passed. This means that the recognition performance is indeed affected. For a more compact and clear comparison of the classifiers, the ROC curve is an appropriate tool. It relates the percentage of correct classifications P_{CC} to the percentage of false alarms P_{FA}. For a well adopted classifier the ROC curve will start at the point {1,1}, then move with a rising threshold close to the ideal point {0,1} corresponding to 100% of correct classification and no false alarm, and finally it drops down to the point {0,0} [3].

Fig. 4a) includes the corresponding ROC curve for the output of classifier C_A in fig. 3a). At a false alarm rate P_{FA} of 1 percent there is a recognition rate P_{CC} of 74 percent. A more detailed analysis by separating the results for heading of the vehicle towards the sensor (table positions between 270° and 90°) and away from the sensor (between 90° and 270°) shows some difference. This is obvious in the ROC curves in fig. 4b.

Looking from the rear we get a P_{CC} of 86 percent for a 1 percent P_{FA}, but only 61 percent P_{CC} for the case illumination from ahead. This can be related to a denser covering on the front part of the vehicle as the photographs show.

a)

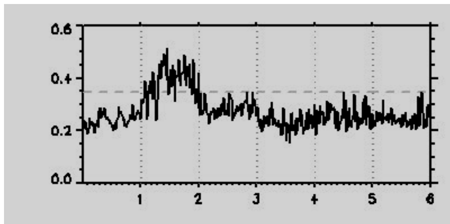

b)

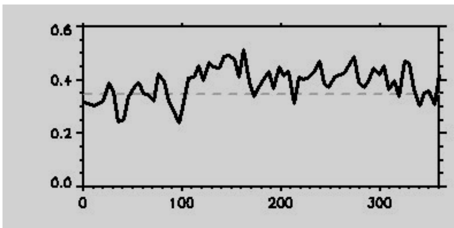

Figure 3: Discrimination values d_A of C_A, a) for 6 scenes, second one: target 'A' covered by birch branches, others: other targets or confusers, b) d_A for scene 2 over 360° in higher resolution. The dashed line represents the threshold for a P_{FA}=0.01.

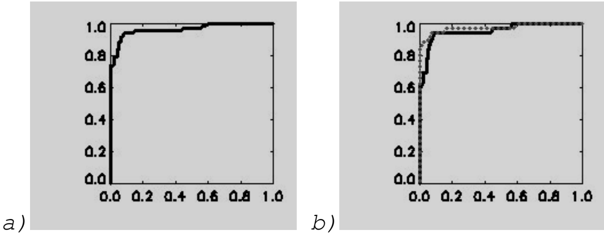

Figure 4: ROC curves for Classifier C_A a) applied on complete scene 2, b) solid for table position between 270° and 90°, dotted for table position between 90° and 270°.

Following example is a smaller armoured vehicle (followingly called type 'B') also covered by birch branches. The photographs, RCS images and filtered images for headings in the cardinal directions are shown in fig. 5 as well as the corresponding training images for the uncovered target. Again, some reductions are recognizable. To estimate the influence of this camouflage on the ATR performance the discrimination values for this scene and for four other scenes with other targets or confuser are evaluated in fig. 6.

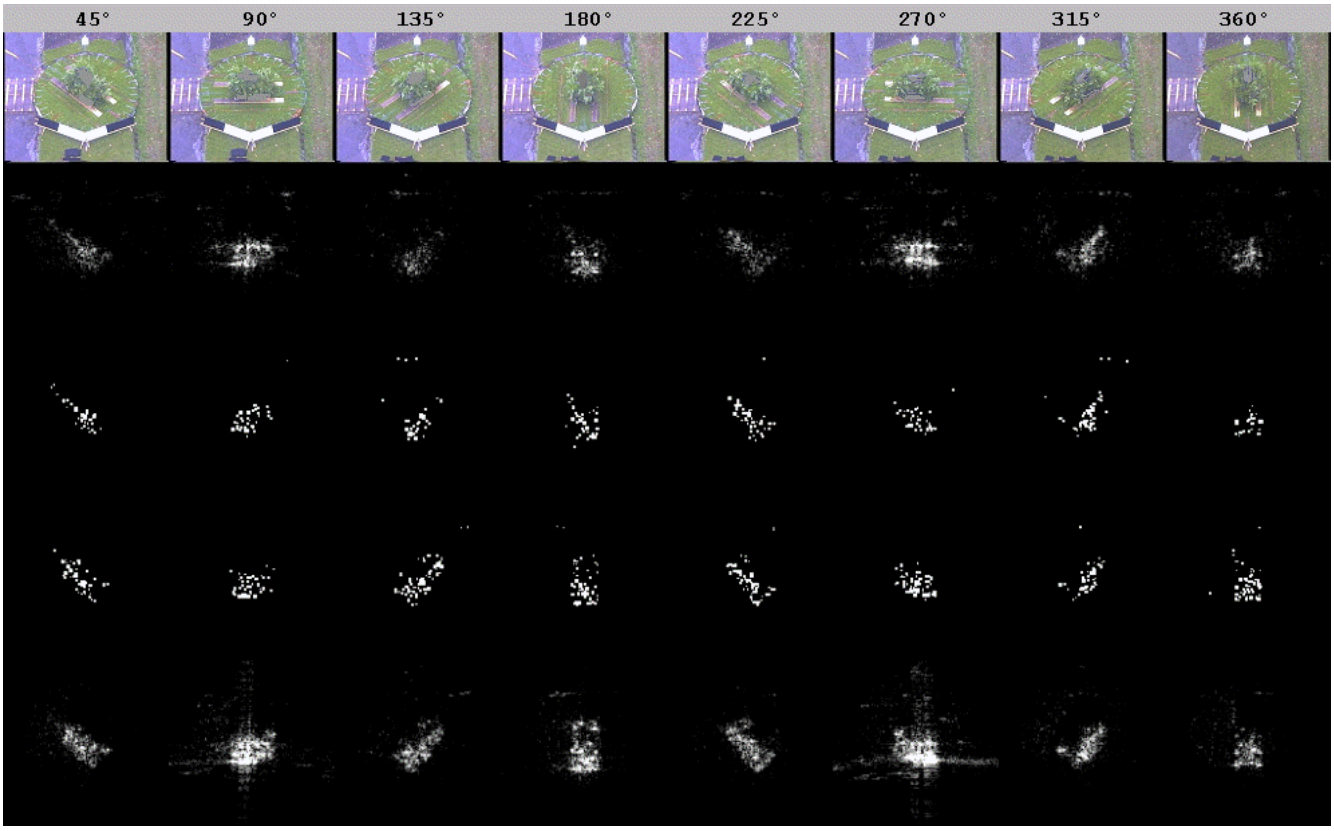

Figure 5: Images of target 'B', a small armoured vehicle covered with birch branches for positions 45°, 90°, 135°, 180°, 225°, 270°, 315° and 360°. First row: photograph (test scene), second row: RCS image of the test scene, third row: ATR relevant digitized image of the test scene, lower second row: digitized image of the training scene (uncovered target), lower row: RCS image of the training scene (uncovered target).

Figure 6: Discrimination values d_B of C_B, a) for 5 scenes, fourth one: target B covered with birch branches, other scenes: different targets or confusers, b) d_B for scene 4 in higher resolution. The dashed line represents the threshold for a P_{FA}=0.01.

The corresponding ROC curve is visible in fig. 7. The P_{CC} for P_{FA}=0.01 is 0.83. A separation of the scene into the sections front/rear part and broadsides towards the sensor is done in fig. 7b. For the broadsides there is a $P_{CC}(P_{FA}$=0.01) of 0.97, meanwhile the P_{CC} drops to 0.5 for the front and rear part. The reason for this behaviour is, that only the upper parts of the vehicle are covered. But uncovered side structures like wheels and chains give good information to the radar ATR system.

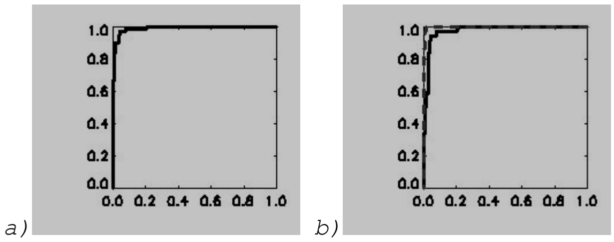

Figure 7: ROC curves for Classifier C_B a) applied on complete scene 4, b) solid: table position from 315° to 45° and from 135° to 225°, dashed: other table positions.

Obviously, there is some potential in hiding a target by natural camouflage against HR X-band radar. But reliable success in camouflaging a military vehicle against radar reconnaissance in the introduced manner requests careful covering of the whole object. From the view of the image analyst, the applied method gives good prospects to recognize a not completely occluded target. Even as in the last introduced example of the small armoured vehicle an optical recognition is likely to fail.

How the ATR performances becomes affected by covering with a net designed against radar sensors, we will discuss in the following section.

3.1.2 Camouflage with radar nets

Fig. 8 illustrates an experiment on target 'B' covered with an artificial radar net. In a separate test this net showed an attenuation of about 25dB in X band. According to this high attentuation we find dramatic differences between the radar images of the test and training scene. The number of resolved scattering centers drastically decreases for the camouflaged target.

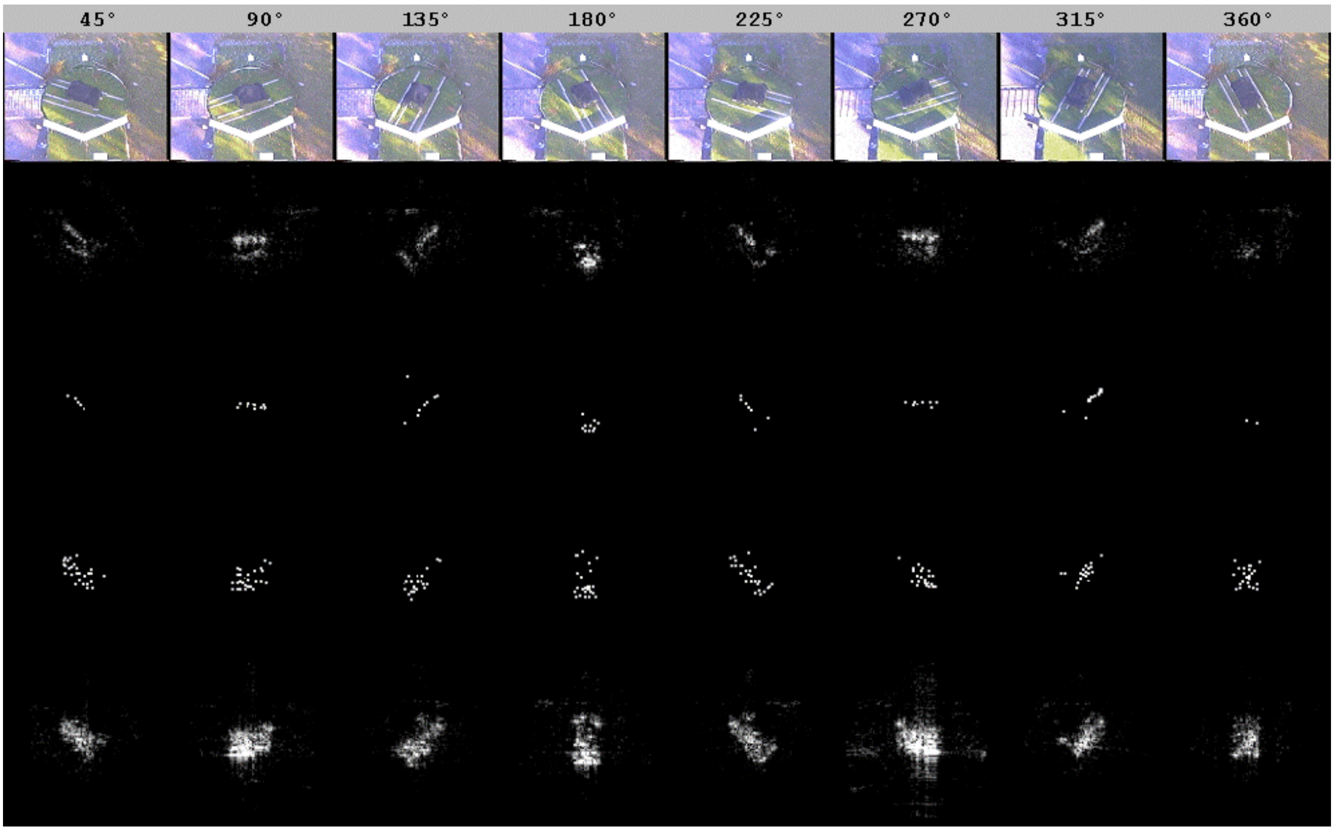

Figure 8: Images of target 'B', a small armoured vehicle covered with a radar net (type '1') for positions 45°, 90°, 135°, 180°, 225°, 270°, 315° and 360°. First row: photograph (test scene), second row: RCS image of the test scene, third row: ATR relevant digitized image of the test scene, lower second row: digitized image of the training scene (uncovered target), lower row: RCS image of the training scene (uncovered target).

The discrimination results of classifier C_A are shown in fig. 9. Scene 5 is the actual one, scene 1 to 4 are other targets or confusers and scene 6 is another scene of target 'B', discussed beneath. Fig. 9b shows a relatively homogenous result for the whole 360° aspect range. The values predominantly lies beneath the P_{FA}=0.01 threshold, which indicates a hardly possible recognition. Not surprisingly, the ROC-curve in fig. 10 reveals a worse ATR performance, - a diagonal in the ROC diagram means a fully stochastic process. The $P_{CC}(P_{FA}=0.01)$ is only 0.1.

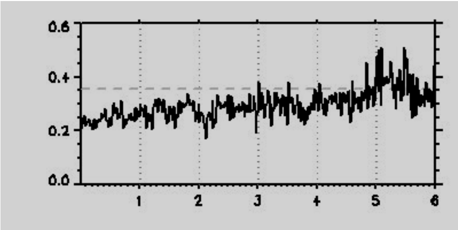

a)

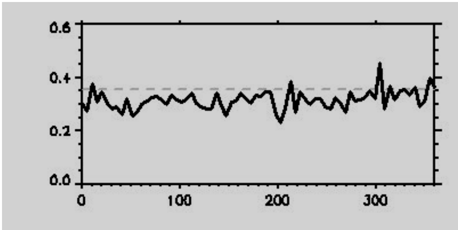

b)

Figure 9: Discrimination values d_B of C_B, a) for 6 scenes, fifth one: target B covered with radar net '1', scene 6: other scene of target 'B', other scenes: different targets or confusers, b) d_B for scene 5 in higher resolution. The dashed line represents the threshold for a P_{FA}=0.01.

Additionaly, we had the possibility to undertake tests with a peace of another type radar net ('2'), but of very limited size. Therefore, we made an experiment in which we only covered the side structures of target 'B', one side with net '2', the other one with the above introduced net '1'.

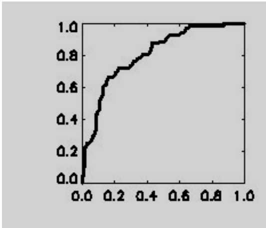

Figure 10: ROC curve for Classifier C_B applied on scene 5.

Net '2' is designed for multiple camouflage tasks, as like against optical, infra-red and radar sensors. In a separate test the attenuation showed a dependence on frequency and polarisation in X-band. In the scene of fig. 11 it was applied to attenuate the radar signal about 20dB.

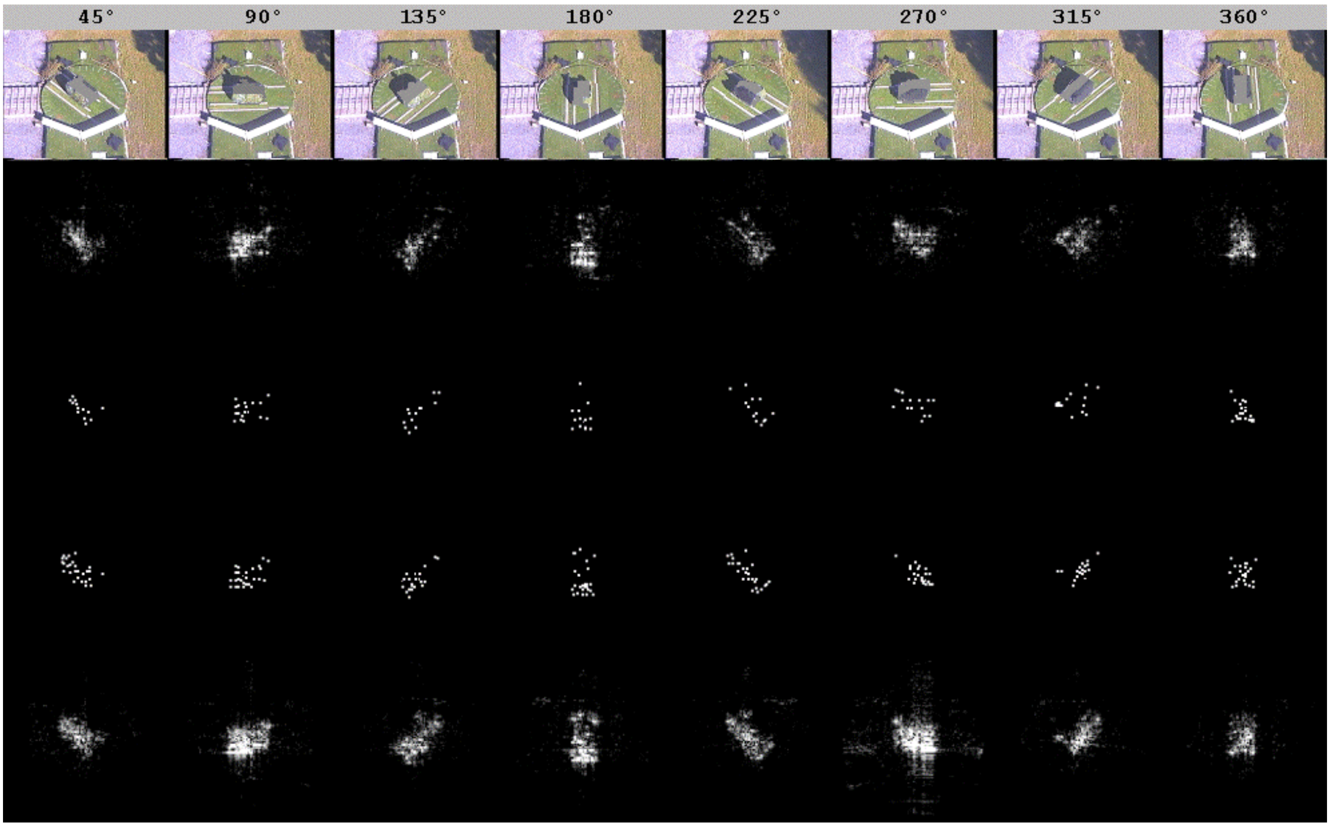

Figure 11: Images of target 'B', a small armoured vehicle partially covered with radar nets (type '1' & '2') for positions 45°, 90°, 135°, 180°, 225°, 270°, 315° and 360°. First row: photograph (test scene), second row: RCS image of the test scene, third row: ATR relevant digitized image of the test scene, lower second row: digitized image of the training scene (uncovered target), lower row: RCS image of the training scene (uncovered target).

There are some reductions recognizable in the radar images of fig. 11, but not as strong as in the last example with net '1' only. Fig. 12 shows the discrimination values. The according ROC curve is drawn in fig. 13a). The $P_{CC}(P_{FA}$=0.01) for the whole scene is 0.5.

Since we applied different nets in this scene we developed 2 ROC curves in fig. 13b) separating the test data set to represent the two nets. The solid line shows the result for the net '2' side, the dashed line belongs to the net '1' line. The $P_{CC}(P_{FA}=0.01)$ for the net '2' side is 0.72, for the net '1' side it is 0.28. The second part tends to the result on net '1' above.

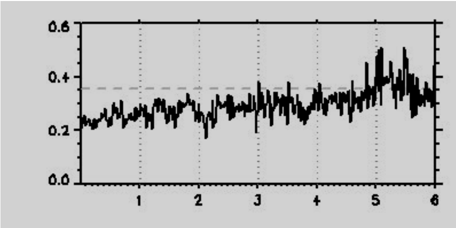

a)

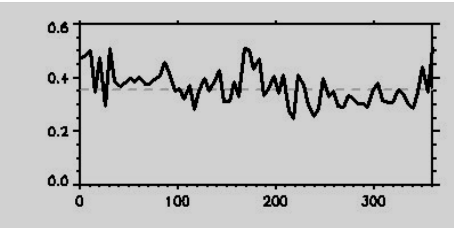

b)

Figure 12: Discrimination values d_B of C_B, a) for 6 scenes, sixth one: target B covered with radar nets '1'+'2', scene 5: other scene of target 'B', other scenes: different targets or confusers, b) d_B for scene 6 in higher resolution. The dashed line represents the threshold for a P_{FA}=0.01.

The first part shows less impact on the ATR performance. Nevertheless, even if the attenuation of net '2' is less, the main reason for the observed results should be found in the rate of occlusion, that is realized by the covering.

For better comparison, fig. 14 combines the results of the introduced camouflages on target 'B'. The solid line represents the 'natural' camouflage (figs. 5-7). The dark grey dashed line stands for camouflage by net '2' and the light grey dashed line for net '1'.

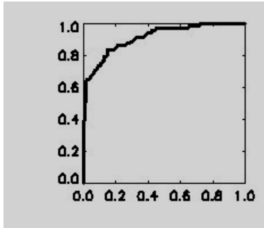

a)

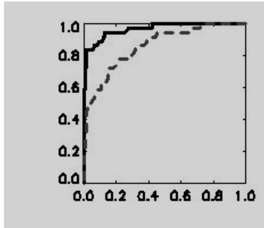

b)

Figure 13: ROC curves for Classifier C_B, a) applied on complete scene 4, b) solid: table position from 315° to 45° and from 135° to 225°, dashed: other table positions.

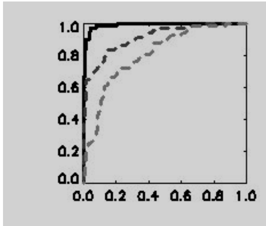

Figure 14: ROC curves for Classifier C_B on camouflaged target B, black solid: 'natural' camouflage, dark grey dashed: net '2', light grey dashed: net '1'.

According to their attenuation on the applied radar signal, the radar nets have massiv effect on the ATR performance. Therefore, they may be a most valuable tool for camouflage against radar reconnaissance.

Besides covering, there is another strategy conceivable. That is interference with the radar signature by adding scattering centers into the scene close to or upon the target. Simmilar effects can be achieved by producing multi-path effects with the ground. Following chapter presents an invstigation of the effects on the ATR performance when the ground is partially covered with metal plates.

3.2 Interference with the radar signature by mutli-path effects

In this section we present results after covering the ground close to the target partially with metal plates. On one hand, these experiments shall give an idea, how robust the radar ATR system reacts on the interfering. On the other hand, they shall show, whether interfering the radar signal by multi-path effects offer an alternative to the above illustrated camouflage methods.

In fig. 15, beneath the front and the right side of target 'C' metal plates cover the ground of the turntable. Especially at position 90° and 360°, when there is the most interfering of the broadsides with the metal plates, the RCS images show a rise-up of sidelobes and artifacts. Additionally, there are traces of recurrences of the radar signal visible in the filtered images at position 45° and 315° according to interactions of the metal plates with the lower structures of the vehicle.

Fig. 16a) shows the discrimination values for classifier C_C on seven scenes. Scene 1 is the one under consideration. Other scenes include another target or confuser. In fig. 16b) the discrimination curve for the current scene is visible in higher resolution. It shows a deep impact at the positions around 90°, when the interfering ground area is biggest.

The corresponding ROC curve is drawn in fig. 17a). As the situation in the current scene changes with the aspect angle, a separation in different aspect sectors is appropriate for an analysis of the respective impacts.

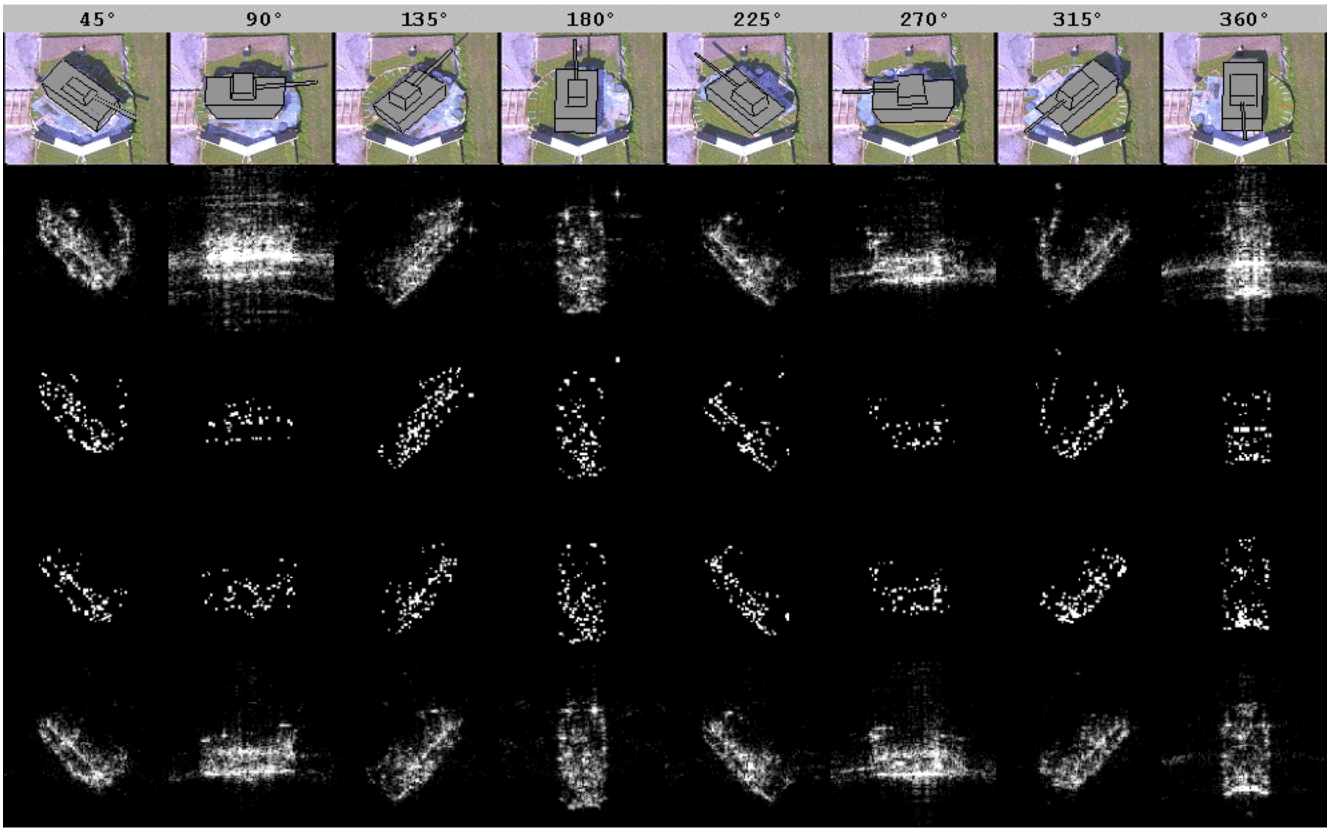

Figure 15: Images of target 'C', partially metal plates on the turntable, for positions 45°, 90°, 135°, 180°, 225°, 270°, 315° and 360°. First row: photograph (test scene), second row: RCS image of the test scene, third row: ATR relevant digitized image of the test scene, lower second row: digitized image of the training scene (target without ground plates), lower row: RCS image of the training scene (target without ground plates).

a)

b)

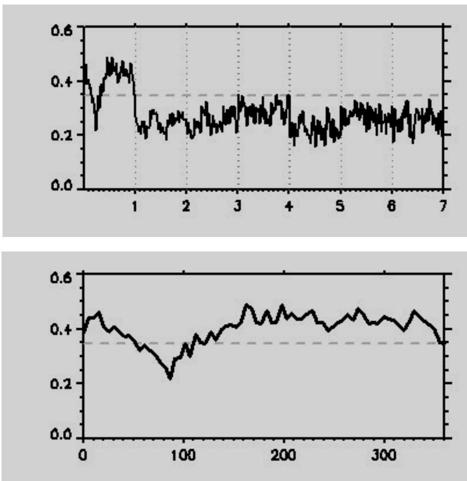

Figure 16: Discrimination values d_C of C_C, a) for 7 scenes, first one: target 'C' plus partially metal plates on the turntable, other scenes: different targets or confusers, b) d_B for scene 6 in higher resolution. The dashed line represents the threshold for a P_{FA}=0.01.

Fig. 17b) shows the ROC curves for a 45° aspect interval around position 90° (dashed light grey), for 45° intervals each around positions 45° and 135° (dotted dark grey), and for the remaining aspect intervals (solid black). The $P_{CC}(P_{FA}=0.01)$ is 0.22 for case 1, 0.78 for case 2, and 0.98 for case 3. These results indicate that there can be an enormous impact on the ATR performance by multi-path effects depending on the degree of coverage of the area next to the target.

a) b)

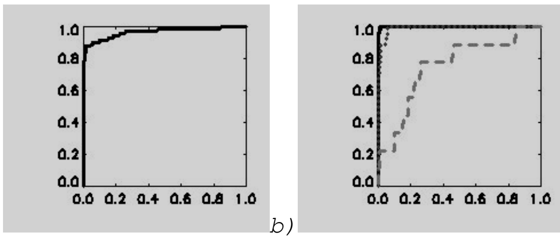

Figure 17: ROC curves for Classifier C_C a) applied on complete scene 1, b) dashed: positions around 90°, dotted: around 45° and 135°, solid: other table positions.

Another experiment with metal plates on the ground and target 'A' is introduced in fig. 18. The plates are placed all around the target, but with lower coverage than in the example above. Fig. 19a) gives the discrimination values of classifier C_A on seven scenes. Scene 2 is under consideration, scene 3 is another target 'A' articulation, remaining scenes include other targets or confusers. In fig. 19b) the disrimination curve for scene 2 is visible in higher resolution.

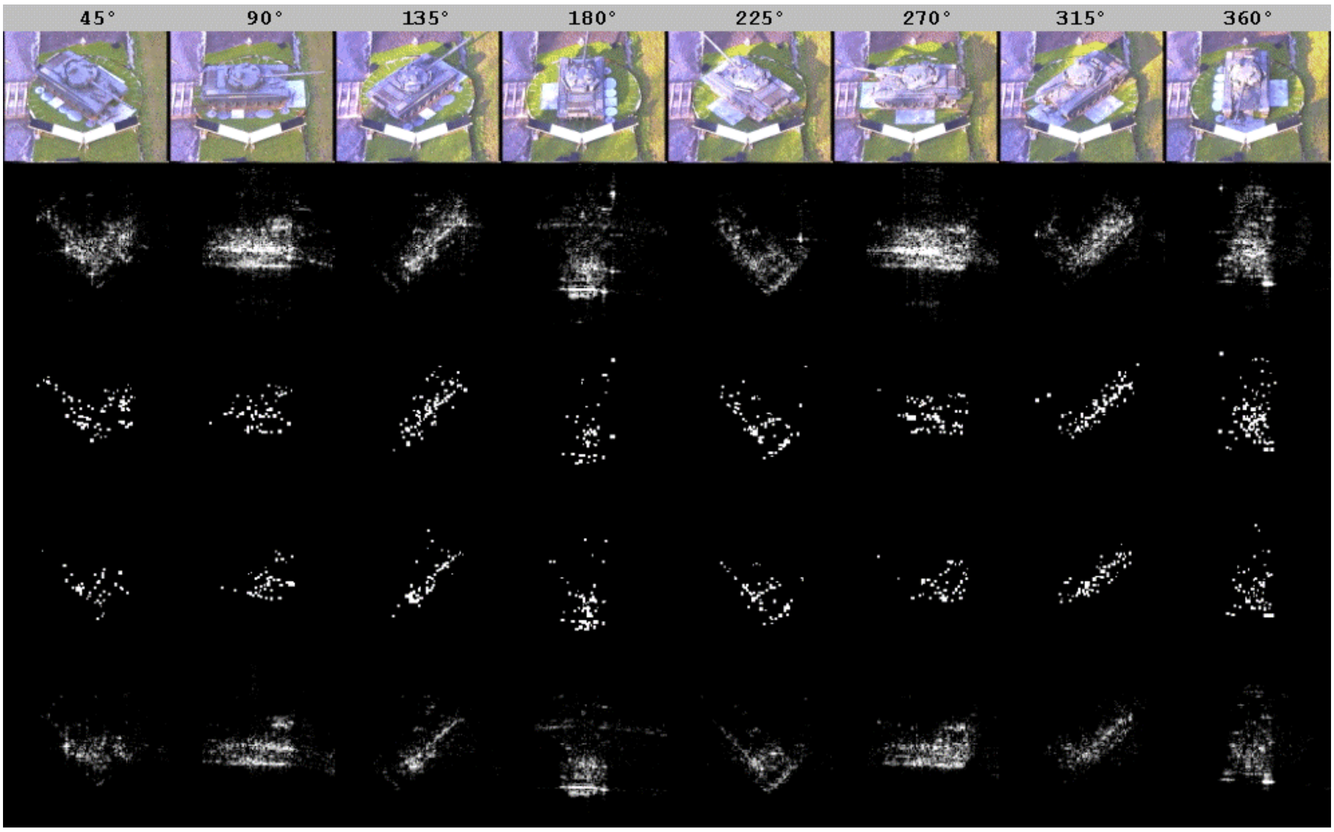

Figure 18: *Images of target 'A', partially metal plates on the turntable, for positions 45°, 90°, 135°, 180°, 225°, 270°, 315° and 360°. First row: photograph (test scene), second row: RCS image of the test scene, third row: ATR relevant digitized image of the test scene, lower second row: digitized image of the training scene (target without ground plates), lower row: RCS image of the training scene (target without ground plates).*

a)

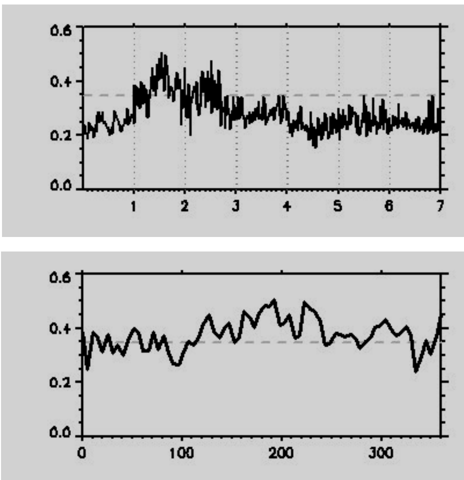

b)

Figure 19: *Discrimination values d_A of C_A, a) for 7 scenes, second one: target 'A' plus partially metal plates on the turntable, scene 3: target 'A' in other articulation, other scenes: different targets or confusers, b) d_A for scene 2 in higher resolution. The dashed line represents the threshold for a P_{FA}=0.01.*

According to the variable covering of the ground there is some difference noticeable for aspects from ahead or from rear the target. This is confirmed by the ROC curves in fig. 20. The black solid curve represents aspects from 112.5° to 292.5°, the grey dotted curve represents the remaining aspects. In the first case we find the $P_{CC}(P_{FA}=0.01)$ = 0.93, for the other one the $P_{CC}(P_{FA}=0.01)$ = 0.62, overall we get a $P_{CC}(P_{FA}=0.01)$ = 0.74.

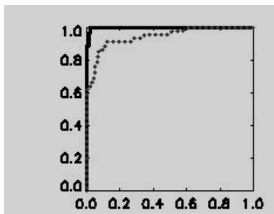

Figure 20: *ROC curves for Classifier C_A applied on scene 2, b) solid: positions between 112.5° and 292.5°, dotted: remaining positions.*

Next example in fig. 21 shows a scene including target 'A', now with a more extensive covering of the surrounding ground area. As like in the corresponding experiment with target 'C' above, in common we can observe an increase of sidelobes and artifacts.

The discrimination values of classifier C_A on seven scenes is shown in fig. 22a). Scene 3 is under consideration, scene 2 includes target 'A' in other articulation, remaining scenes contain other targets or confusers. The discrimination graph of scene 3 is in higher resolution in fig. 22b). In fig. 23 the respective ROC curve is presented (dashed). The $P_{CC}(P_{FA}=0.01) = 0.4$. The ATR performance is noticeably affected. For comparison, the ROC curve for the example above (complete scene) with less coverage on the ground is shown (solid), too.

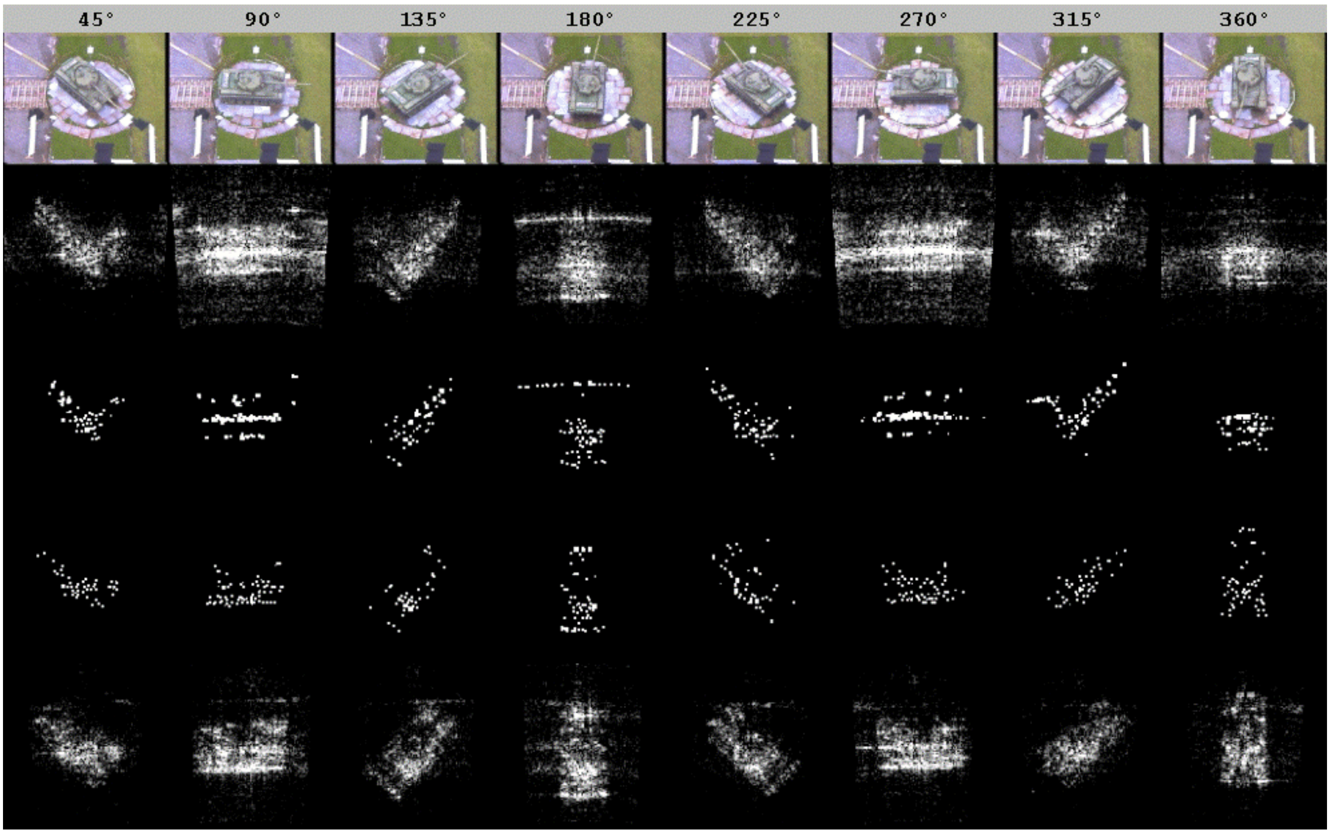

Figure 21: Images of target 'A', metal plates on the turntable, for positions 45°, 90°, 135°, 180°, 225°, 270°, 315° and 360°. First row: photograph (test scene), second row: RCS image of the test scene, third row: ATR relevant digitized image of the test scene, lower second row: digitized image of the training scene (target without ground plates), lower row: RCS image of the training scene (target without ground plates).

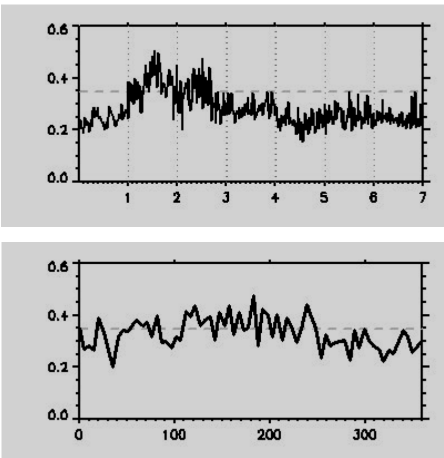

a)

b)

Figure 22: Discrimination values d_A of C_A, a) for 7 scenes, third one: target A plus metal plates on the turntable, scene 2: target A in other articulation, other scenes: different targets or confusers, b) d_A for scene 3 in higher resolution. The dashed line represents the threshold for a $P_{FA}=0.01$.

The assumption, that the degree of coverage determines the impact on the ATR performance becomes supported if we look on fig. 24. There are the ROC curves for the above studied cases for multi-path effects, regarding the separations for different coverage also within one scene. The lighter the curve, the higher is the density of the ground coverage by the metal plates. The denser the coverage, the more we find an affected recognition performance.

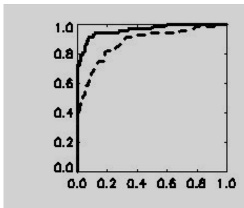

Figure 23: ROC curves for Classifier C_A applied on scene 3 (dashed), solid: scene 2 (example above).

Some difference we find in different targets, as target 'C' showes some more sensitivity than target 'A'. The main reason is, that it has higher side structures. These side structures contain information, which becomes interfered by the reflections on the ground plates.

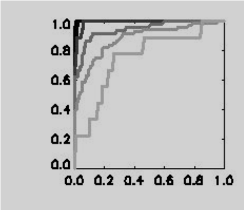

Figure 24: ROC curves for Classifier C_A and C_B applied on scenes with different degrees of ground coverage by metal plates, light: high coverage, dark: less coverage.

The regarded experiments show, that indeed a reflecting ground can influence the ATR performance. Future investigations have to show, whether a ground like concrete can cause similar effects.

Complementarily, an experiment with a decoy is introduced, as this kind of deception is related to camouflage in military practise.

3.3 Deception by a decoy

In one of our last campaigns we had the opportunity to illuminate a decoy that was designed for optical and infra-red deception. As we are not trained for, it was not possible for us to recognize the difference between real target and decoy by eye in a distance of 100m or more. Fig. 25 shows the radar images of the decoy and of its real model. The RCS signature is lower than that of the origin target, and less scattering centers are resolved.

The discrimination values of the corresponding classifier trained on the real target is presented in fig. 26a). The classifier was applied on five scenes, scene 4 contains the decoy. The discrimination values for scene 4 are visible in higher resolution in fig. 26b). The graphs indicate no recognition at all. The ROC curve in fig. 27 confirms that. It is very close to the diagonal as it is for a complete stochastic process. The $P_{CC}(P_{FA}=0.01) = 0.03$.

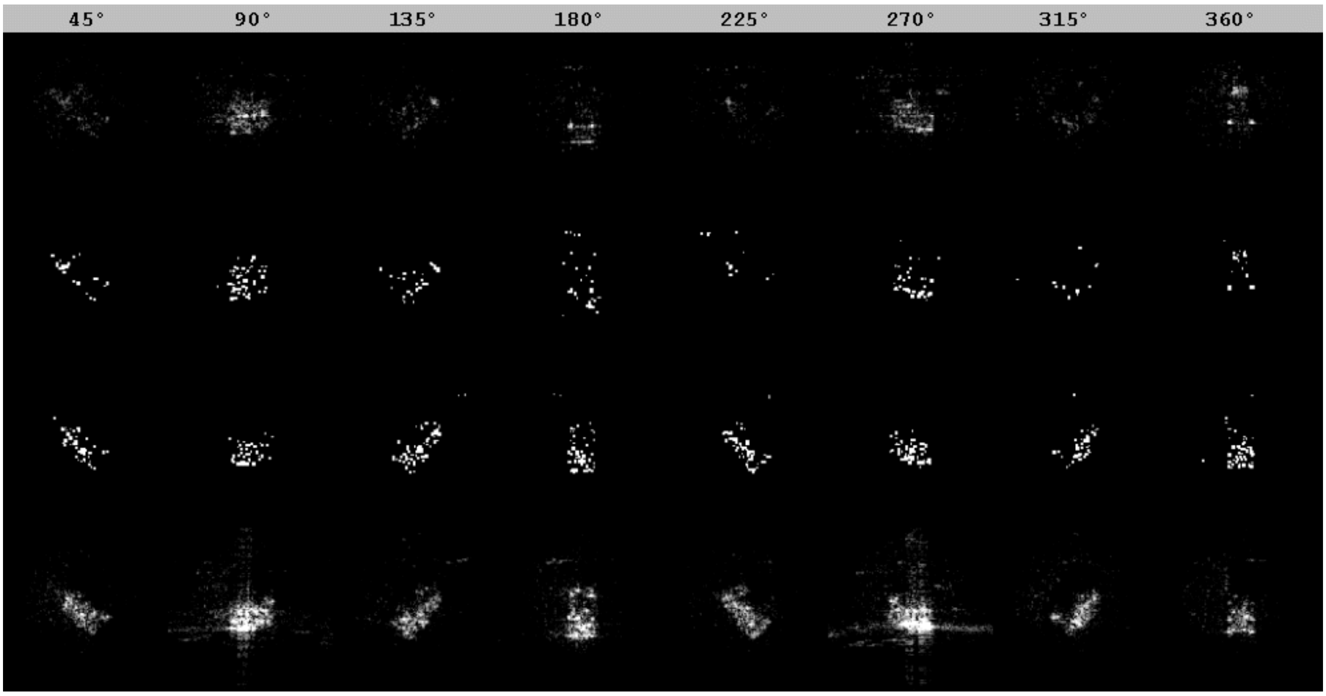

Figure 25: Images of a decoy designed for optical and infra-red application, for positions 45°, 90°, 135°, 180°, 225°, 270°, 315° and 360°. First row: RCS image of the test scene, second row: ATR relevant digitized image of the test scene, lower second row: digitized image of the training scene (original target), lower row: RCS image of the training scene (original target).

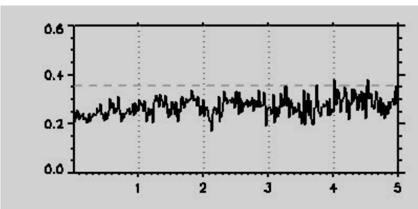

a)

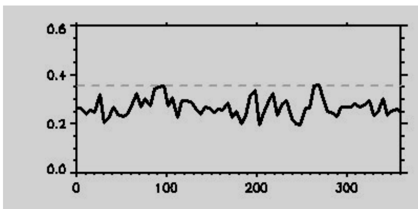

b)

Figure 26: Discrimination values d_X of a classifier trained on original model for the decoy, a) for 5 scenes, fourth one including the decoy, b) d_X for scene 4 in higher resolution. The dashed line represents the threshold for a P_{FA}=0.01.

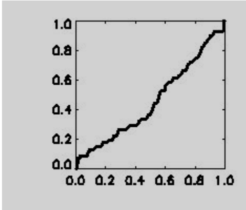

Figure 27: ROC curve for Classifier C_X (trained on origin target) applied on scene 4, containing the decoy.

As it could be expected, the decoy that was not designed for radar applications delivered no radar images comparable to those of the origin target. The RCS values are different and most notably the local distributions of the scattering centers are completely different. In this sense, the radar system cannot be deceived by this kind of decoy.

4. Conclusions

Based on data sets of ISAR tower-turntable measurements, this paper showed the potential effect of some different camouflage methods on the ATR performace of a HR X band radar system.

Camouflage by covering the target with birch branches was as well tested as occlusion by radar nets. Of course, a significant attenuation of the radar signal by the coverage of the target is precondition for affecting the ATR performance. This given, the degree of occlusion determines the impact on the reconnaissance, or on the contrary, the applied ATR system shows a good robustness, if the target is only partially occluded.

Additionaly, tests were undertaken to investigate the influence of multi-path effects by a reflecting ground. Here also, a remarkable affect on the ATR performance could be observed, depending on the degree of coverage of the target surrounding area.

Finally, for complementary a decoy designed for optical and infra-red application was tested with a classifier trained on the origin target. There, no deception of our ATR system could be observed.

References

[1] Kempf, T., and M. Peichl, "ATR Performance within an extended X-band Tower-Turntable Database of highly resolved relocatable targets", Proc. of RTO SET 080 Symposium, Oslo, Norway, Oct. 2004.

[2] Kempf, T., and M. Peichl, "A Method for Advanced Automatic Recognition of Relocatable Targets ", Proc. of RTO SET Panel, Prague, Czech Republic, Apr. 2002.

[3] R.A. English, "Classifier Evaluation Methodology using MSTAR Public Data Set", NATO working paper, DRDC Ottawa, Feb. 2003.

Influence of Camouflage on the ATR Performance for highly resolved ISAR images

Timo Kempf, Markus Peichl, Stephan Dill, Helmut Süß

German Aerospace Center

Microwaves and Radar Institute
Postfach 1116
82230 Weßling, Germany
e-mail: timo.kempf@dlr.de

Oberammergau, May/10/2005

Overview

- Background, data acquisition and imaging.
- ATR method and performance evaluation.
- Tests on camouflaged targets.
  - birch branches, radar net, interfering ground
- Test on a decoy.
  - (designed for optical and infra-red applications)
- Conclusions.

Data acquisition

Equivalence of Spotlight SAR and Turntable ISAR

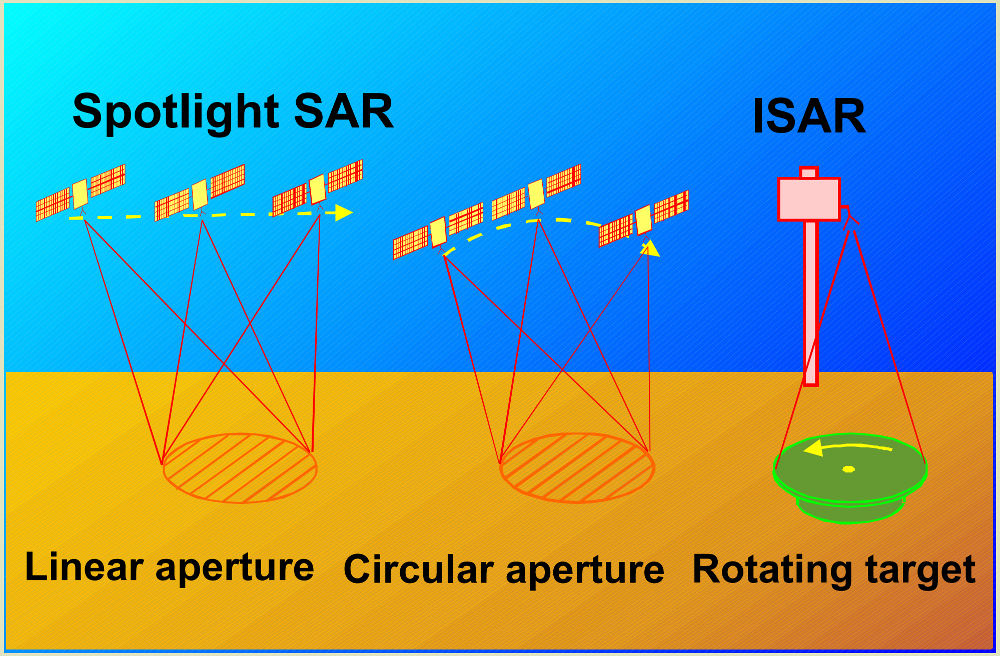

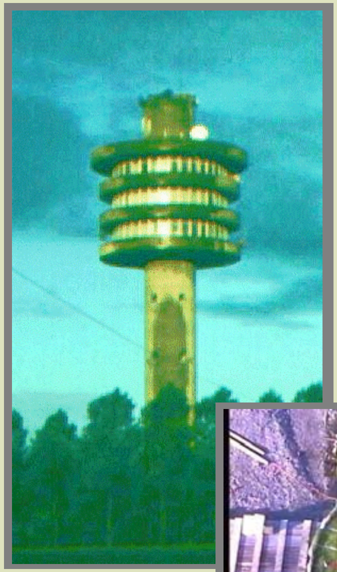

Stepped frequency measurements on a Tower-turntable arrangement

- Enables collection of highly resolved signatures of relocatable targets comparable to those to be expected by a space borne spotlight SAR.

Distance:	60m
Incidence angle:	42.5°, 45°, 47.5°, 50°
Turntable Ø :	9m

Extraction of robust scattering centers

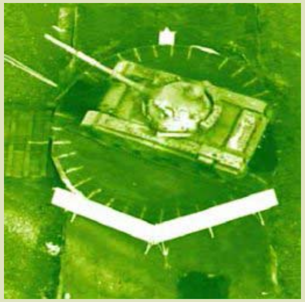

Incoherent superposition for a whole 360° rotation by a projection-on-several-planes-technique.

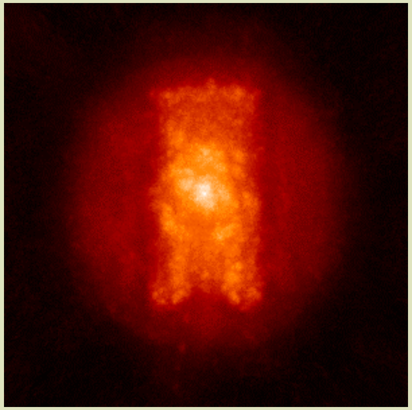

Highly resolved RCS image

(X band)

Sidelobe suppression

Phase analysis

Digitisation

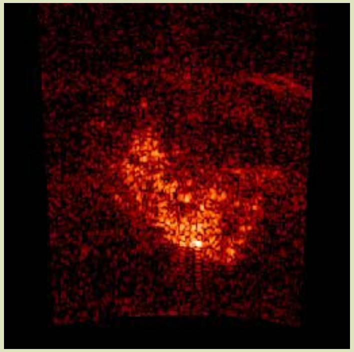

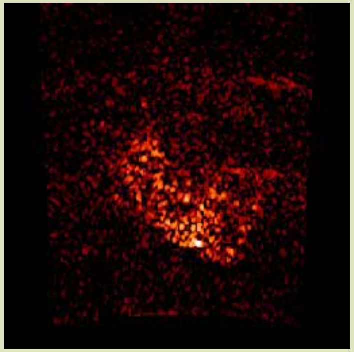

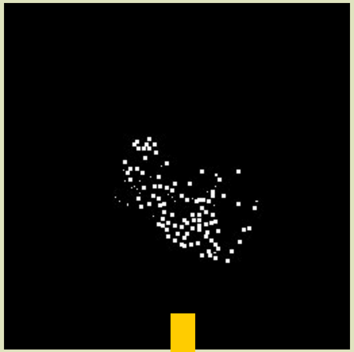

Test/Training Data base

Recognition method

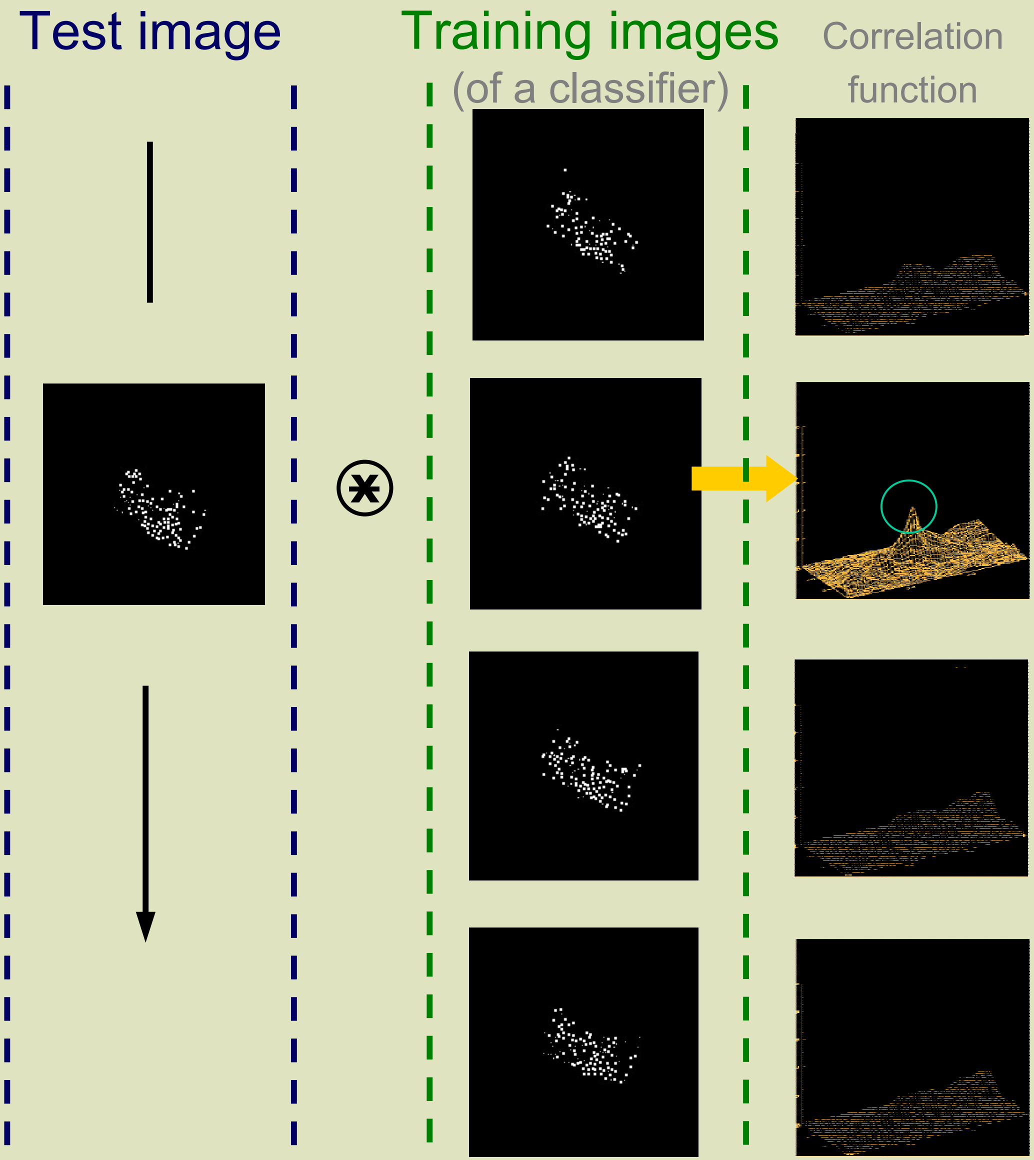

Template matching

Result: For each test image and each classifier maximum correlation value.

Classifier Performance Evaluation

Example: Classifier of a battle tank.

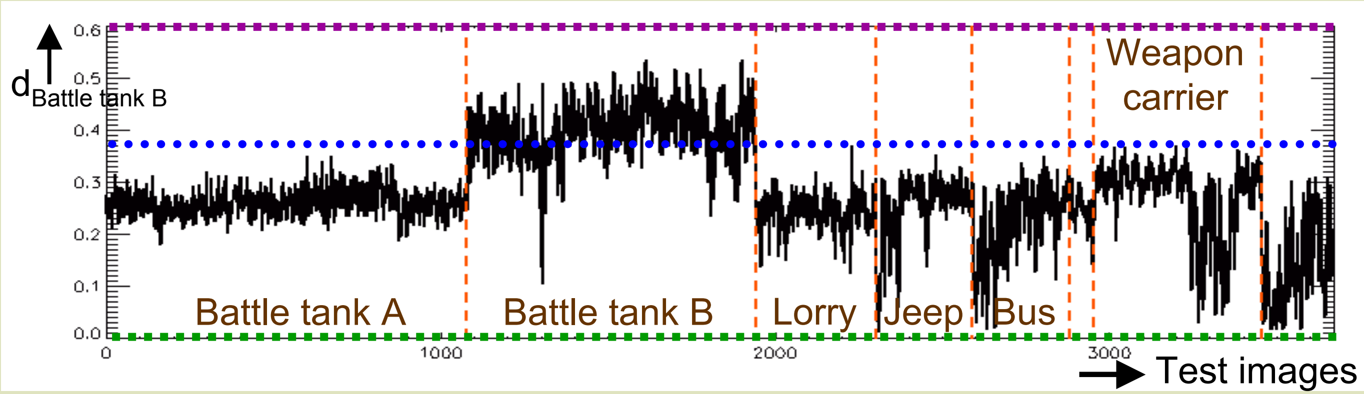

Receiver Operating Characteristic - Curve
(ROC-Curve)

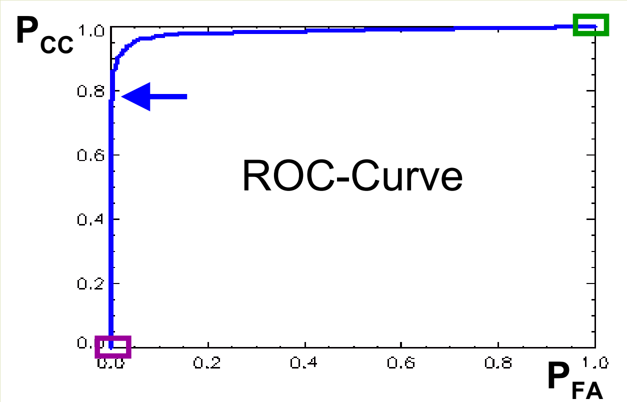

Camouflage: Birch branches

Experiment A — Attenuation of radar signal: ~10dB

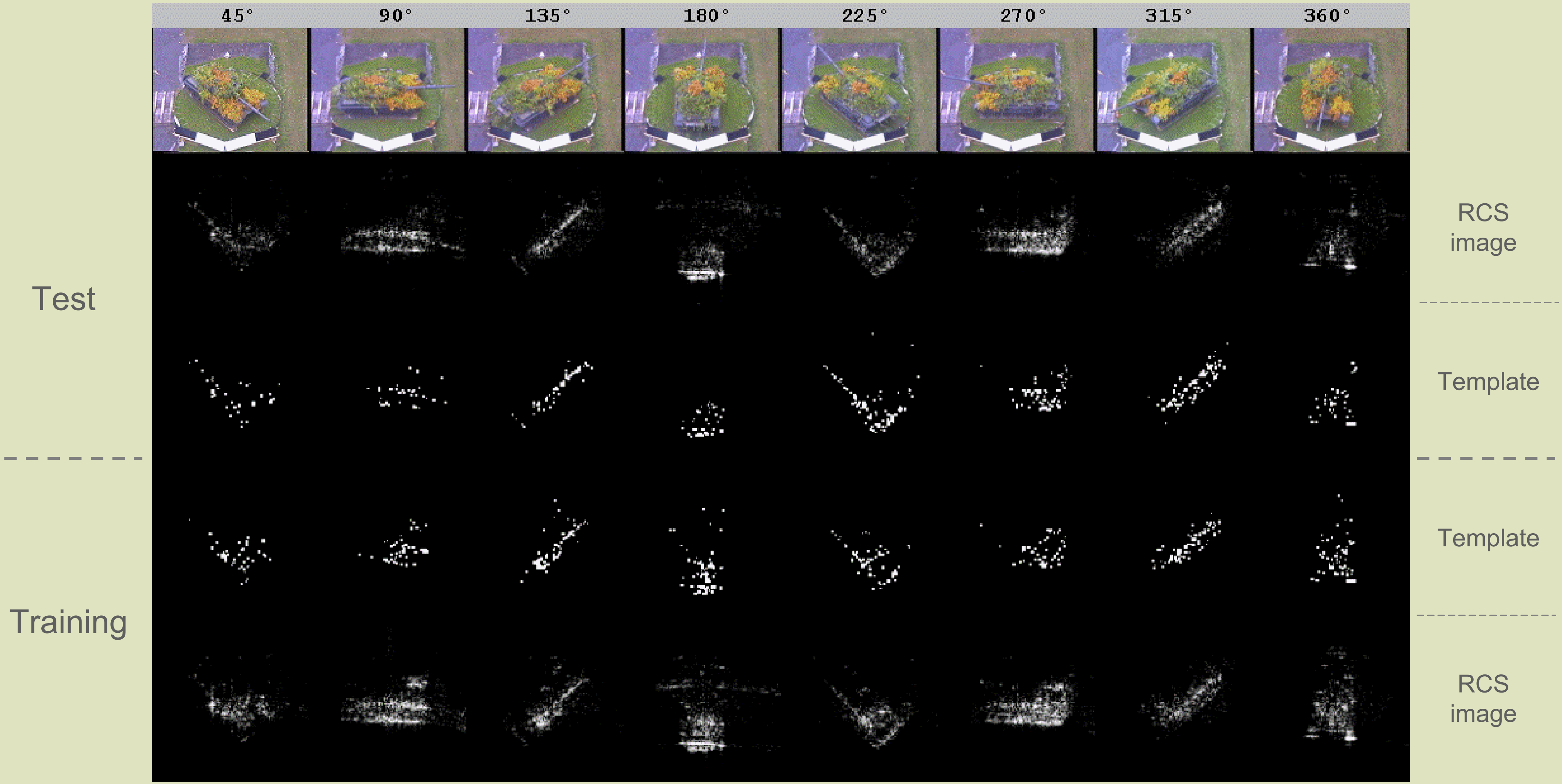

• Reduced SNR • Partially less exctracted scatterers

Camouflage: Birch branches

Experiment A, evaluation

Classifier outcome:

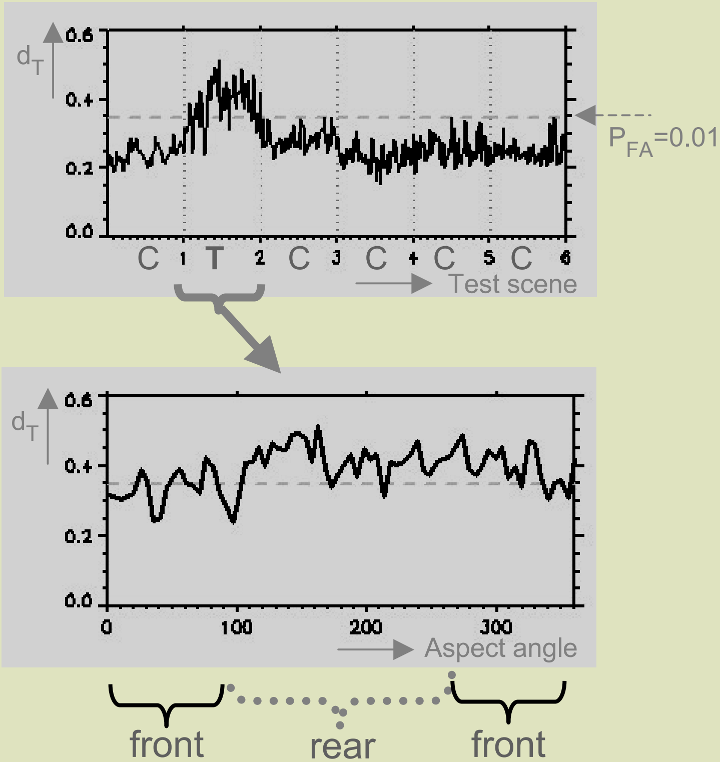

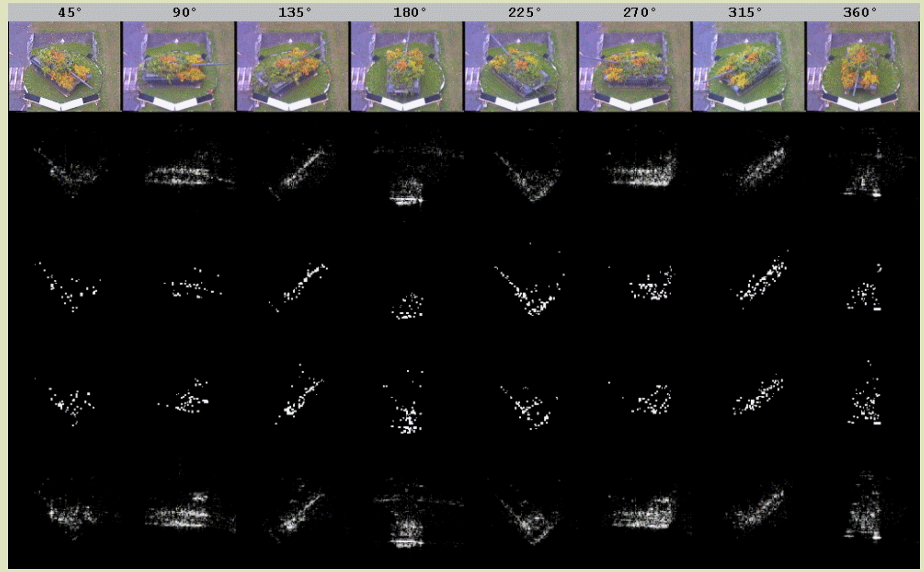

ROC curve, complete scene

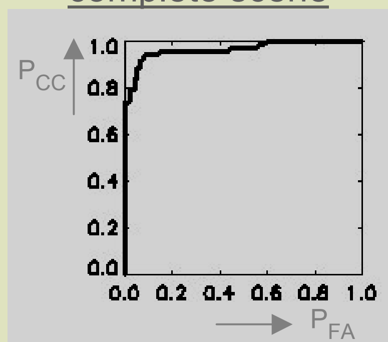

ROC curves, sectors rear/front

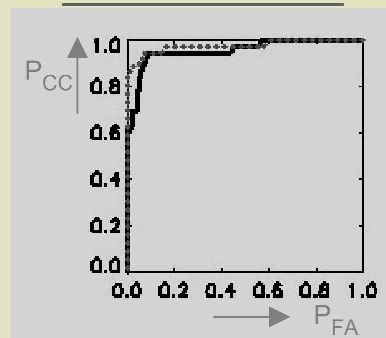

- ATR performance affected
- Depending on rate of occlusion

Camouflage: Birch branches

Experiment B

Attenuation of radar signal: ~10dB

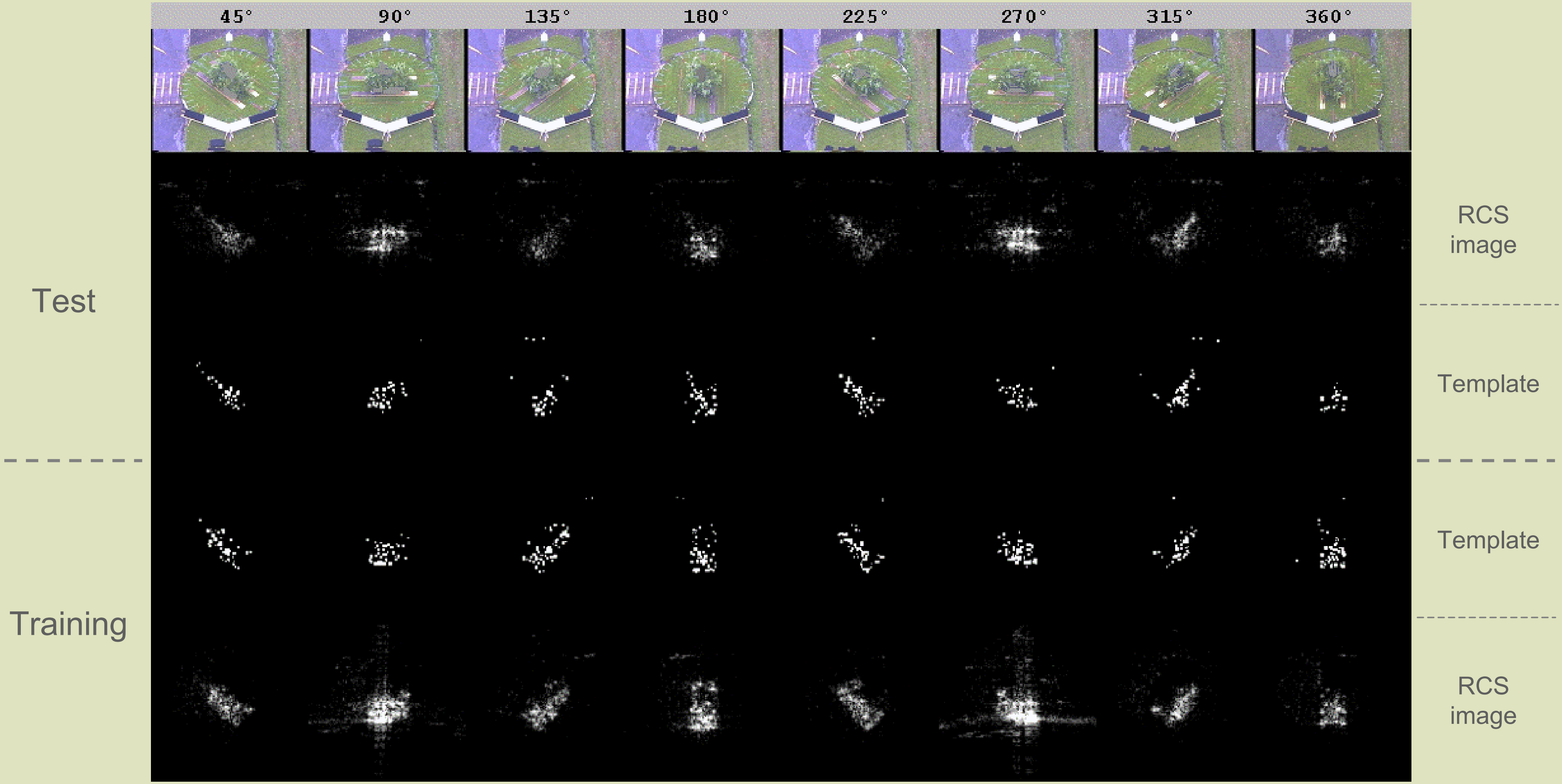

• Reduced SNR • Partially less exctracted scatterers

Camouflage: Birch branches

Experiment B, evaluation

Classifier outcome:

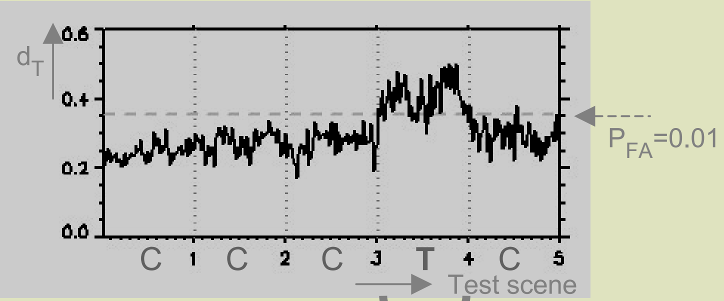

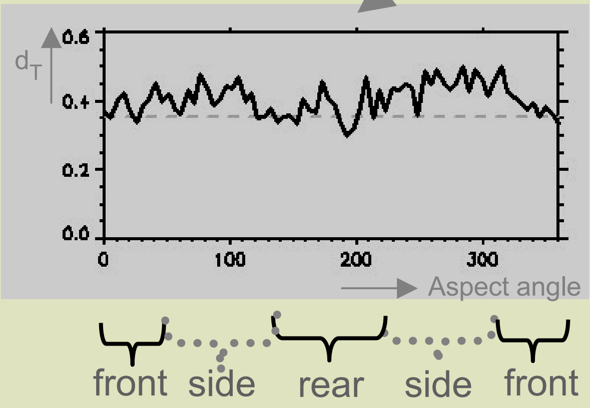

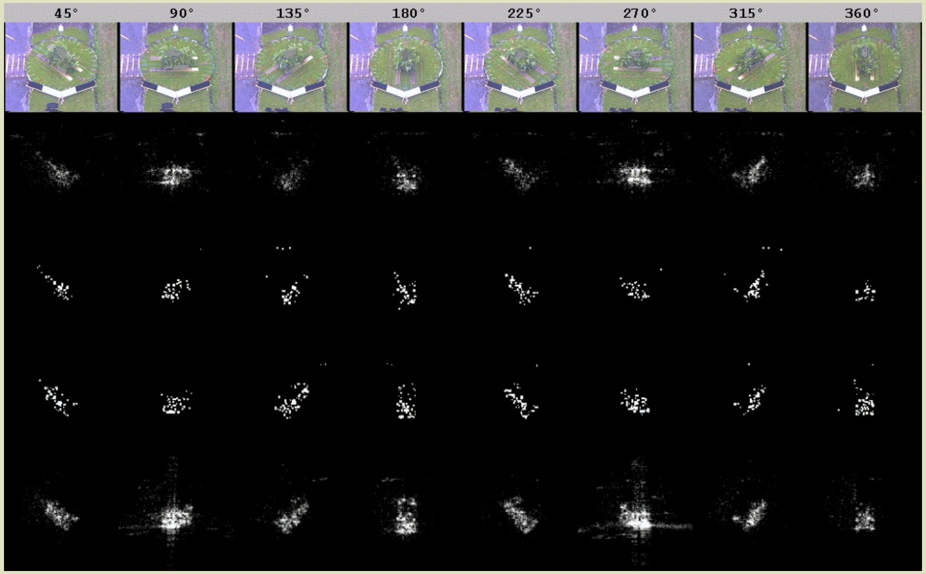

ROC curve, complete scene

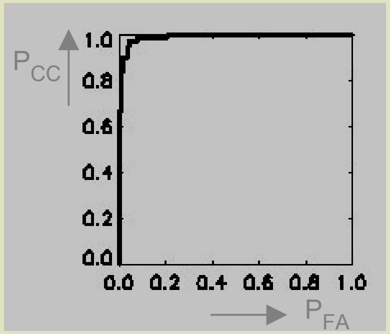

ROC curves, sectors rear&front/sides

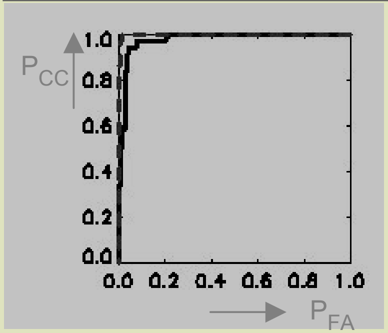

- ATR performance affected
- Depending on rate of occlusion

Camouflage: Radar net

Experiment C

Attenuation of radar signal: ~25dB

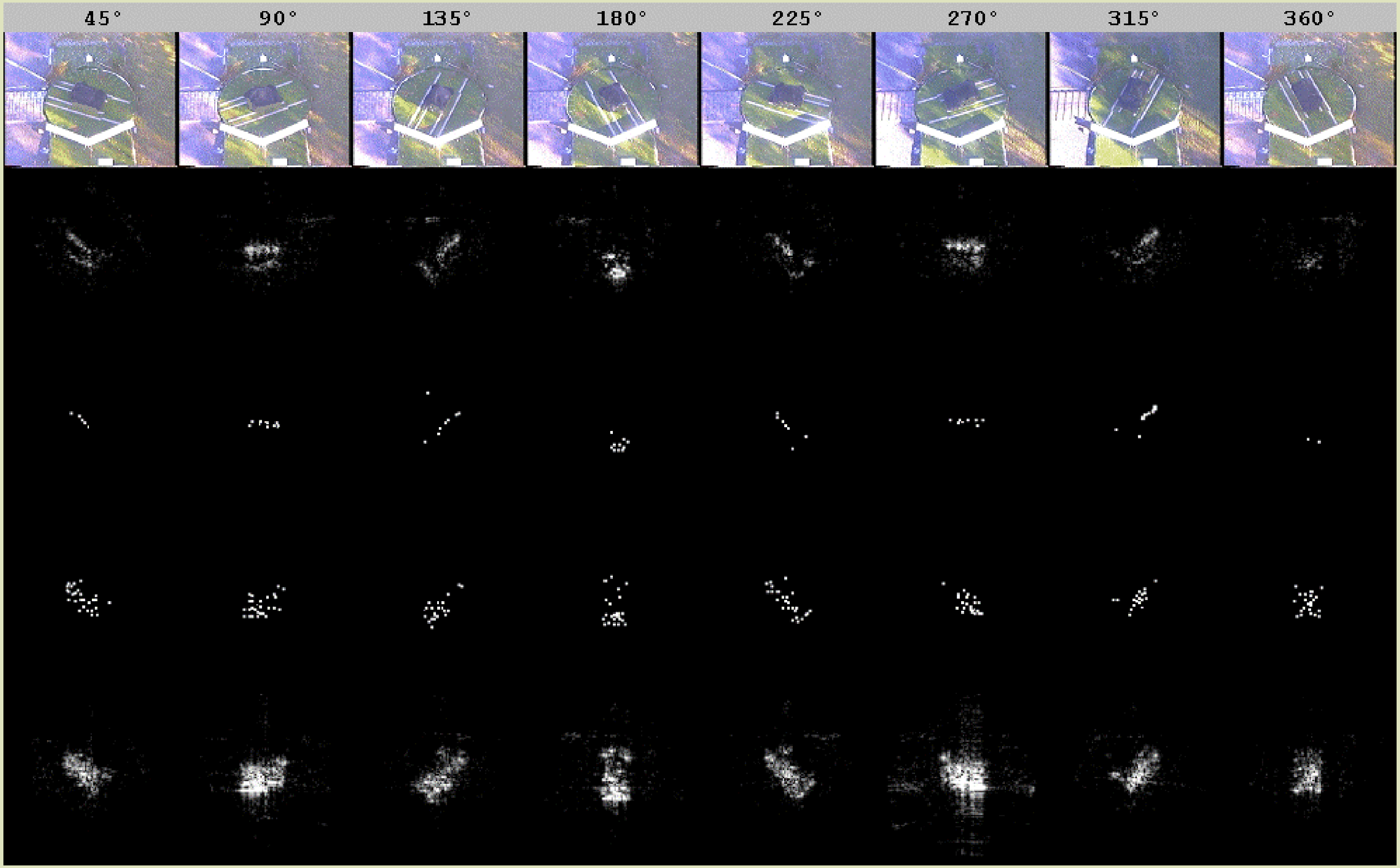

Test

Training

RCS image

Template

Template

RCS image

• Heavily reduced SNR • Low number of exctracted scatterers

Camouflage: Radar net

Experiment C, evaluation

Classifier outcome:

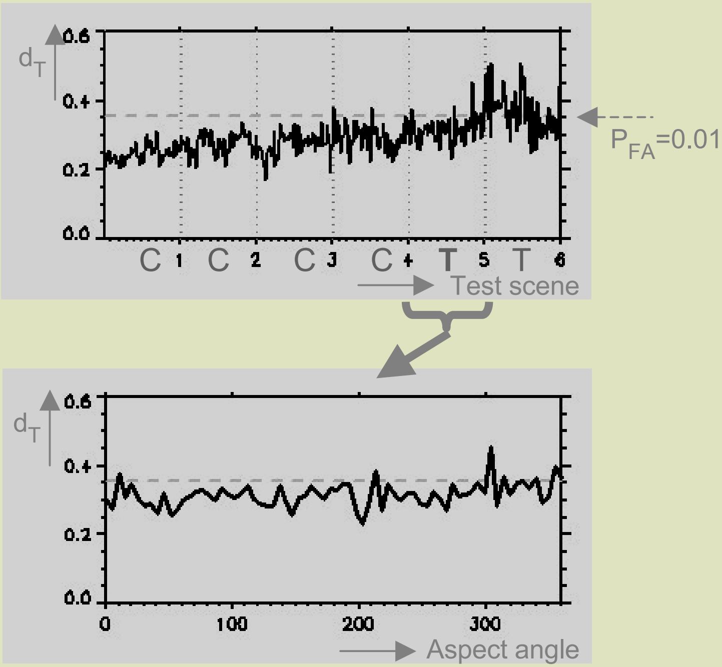

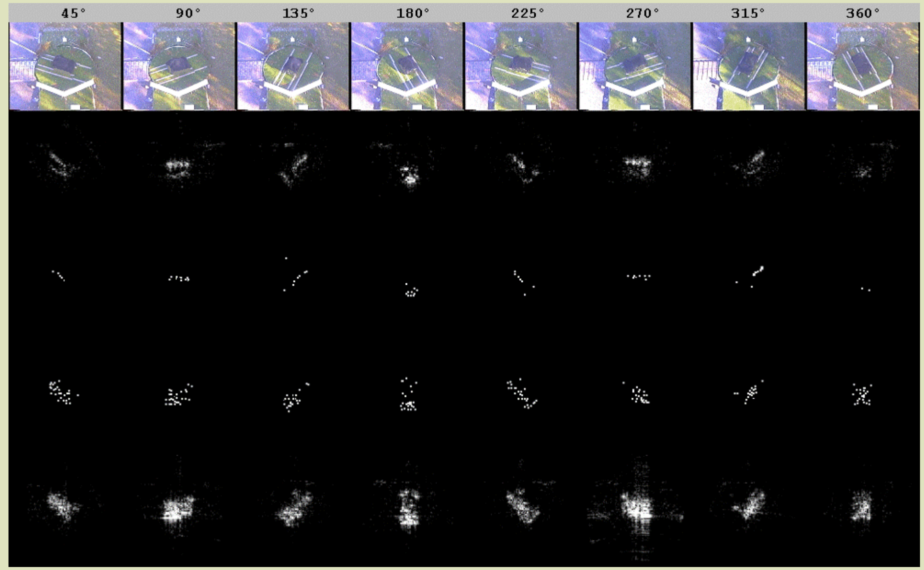

ROC curve, complete scene

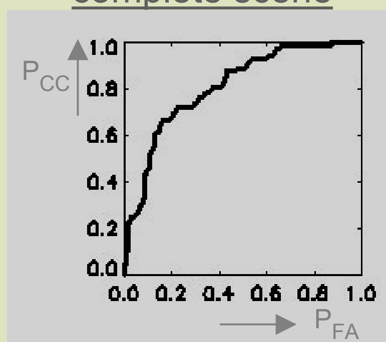

ROC curves, branches/radar net

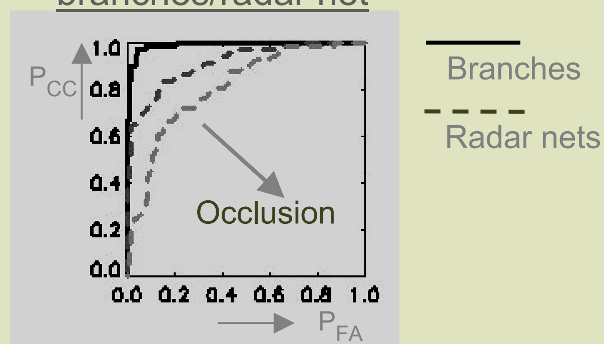

- ATR performance heavily affected
- Depending on rate of occlusion

Interference by multi-path effects

Experiment D — Metal plates beneath front and right side

Test

Training

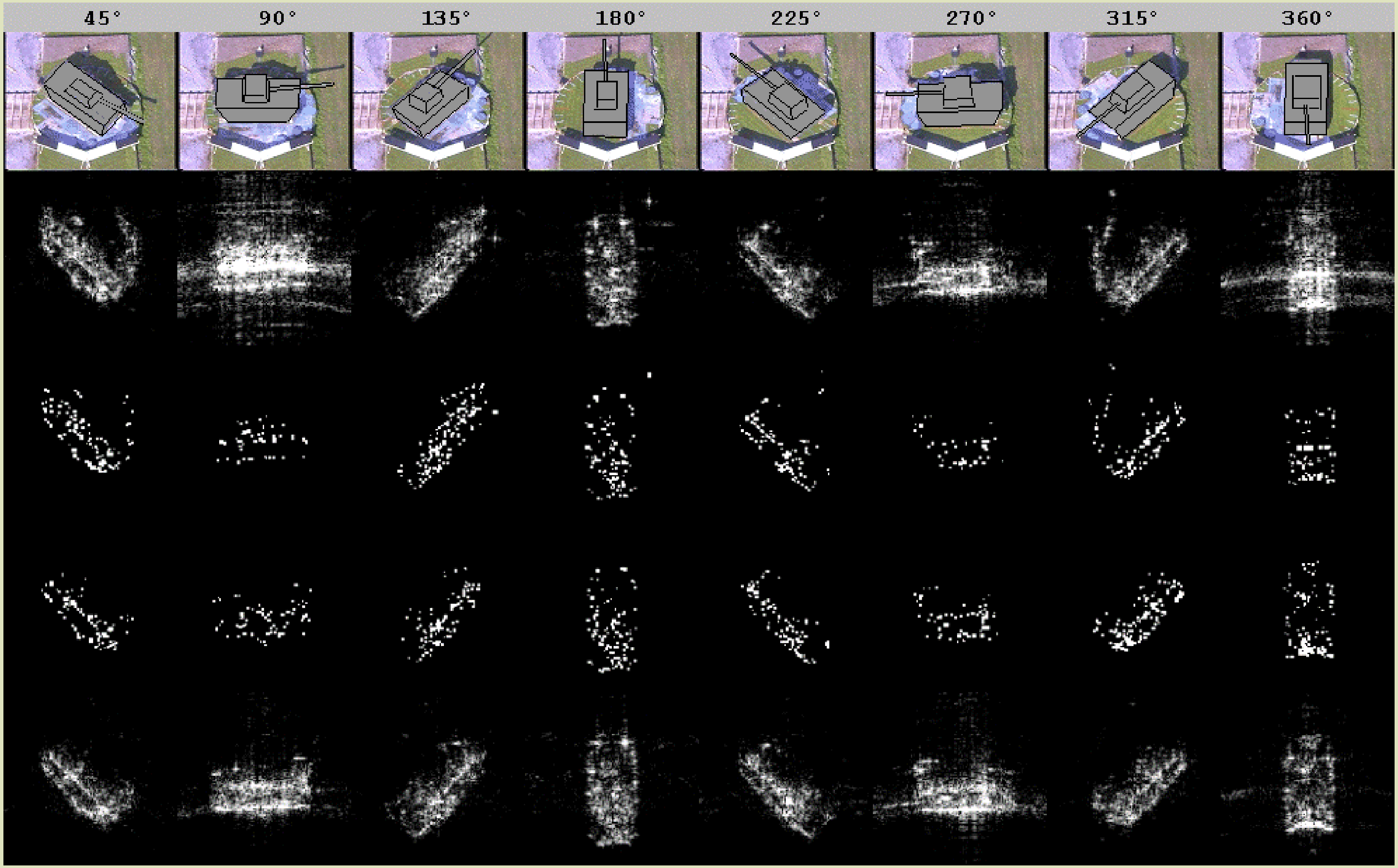

RCS image

Template

Template

RCS image

- Increase of sidelobes and artifacts
- Partially recurrences

Interference by multi-path effects

Experiment D, evaluation

Classifier outcome:

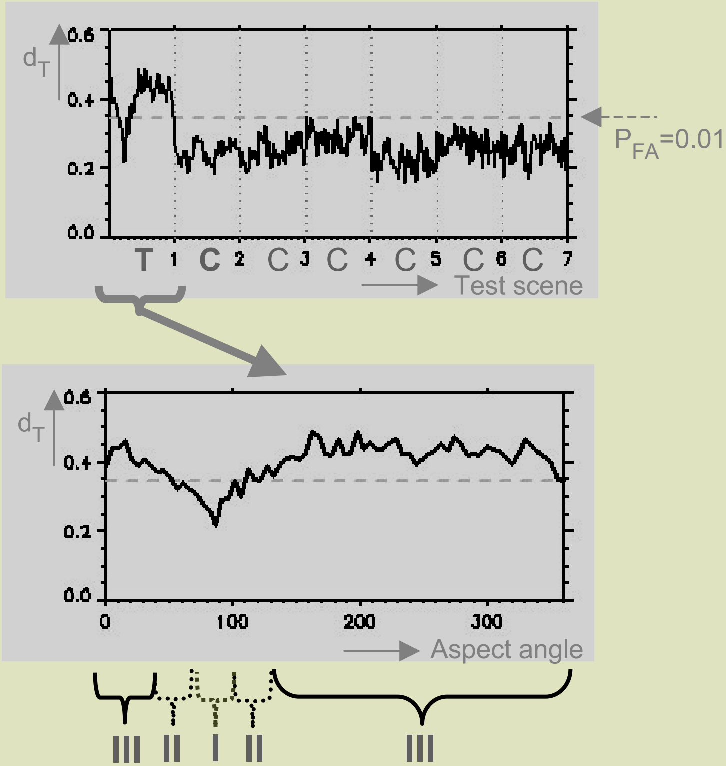

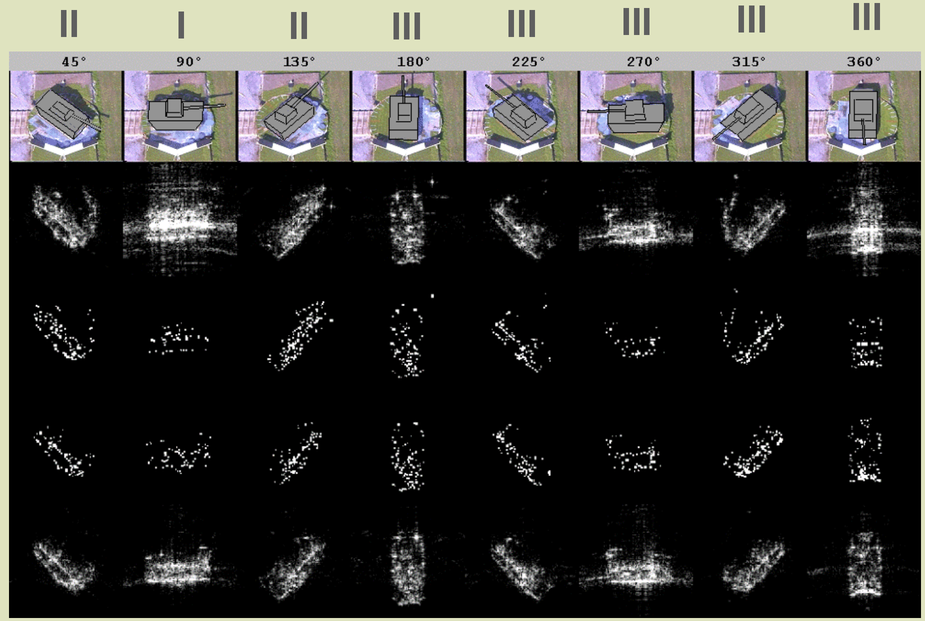

ROC curve, complete scene

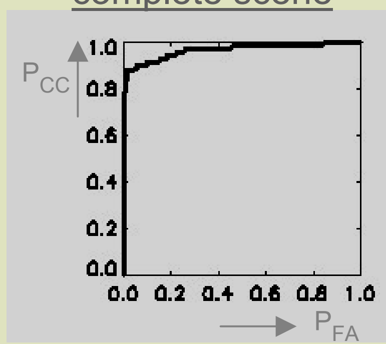

ROC curves, sectors I,II,III

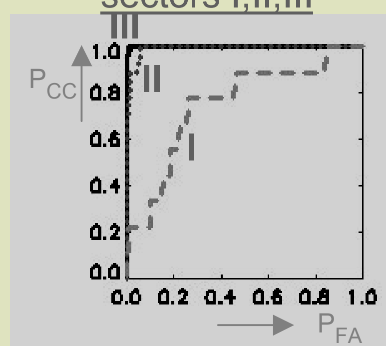

- ATR performance affected
- Depending on rate of ground coverage

Interference by multi-path effects

Experiment E — Metal plates all around

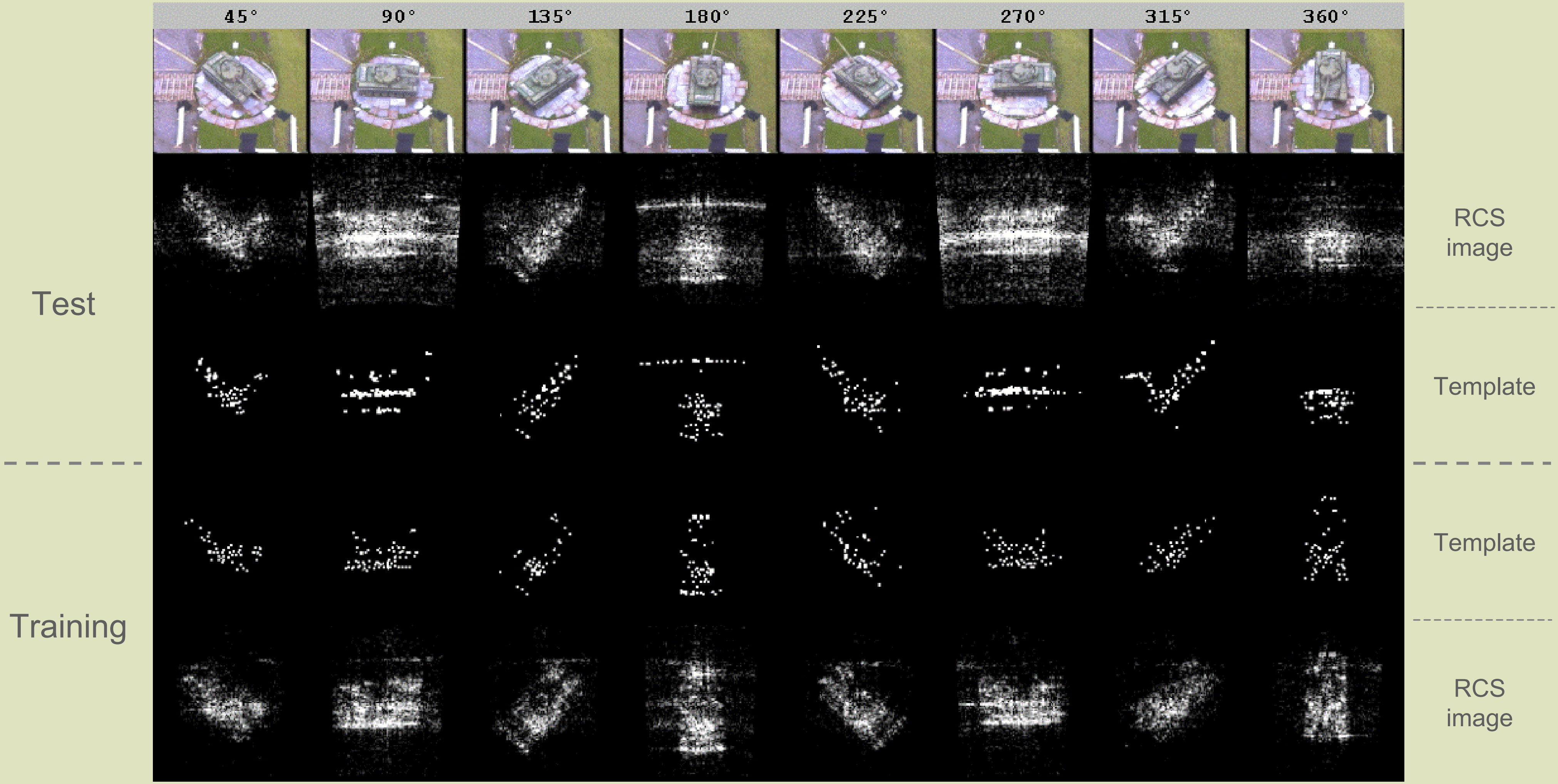

- Increase of sidelobes and artifacts
- Partially more extracted scatterers

Interference by multi-path effects

Experiment E, evaluation

Classifier outcome:

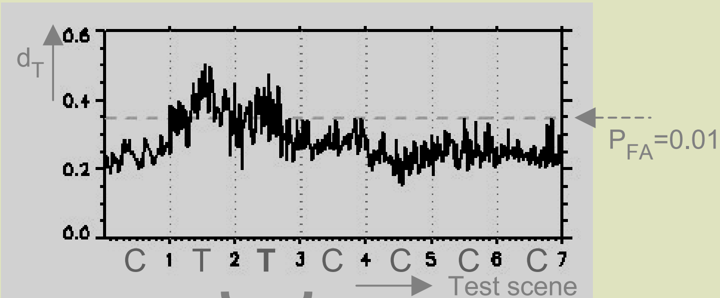

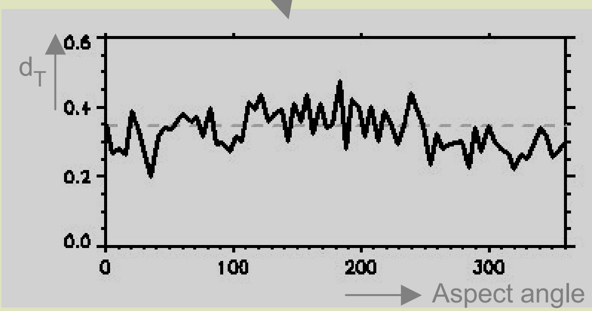

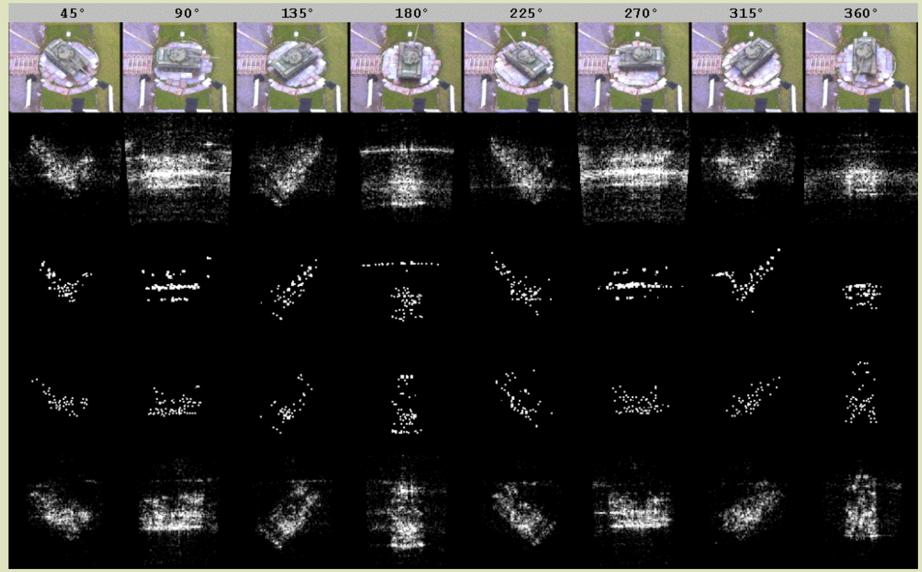

ROC curve, complete scene

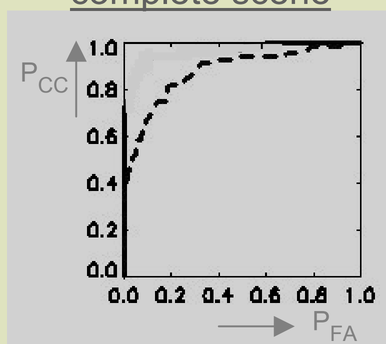

ROC curves, ground coverage

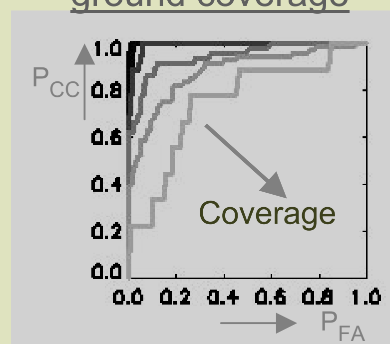

- ATR performance affected
- Depending on rate of ground covering

Deception by decoy

Experiment F

Designed for optical and infra-red applications

Test

Training

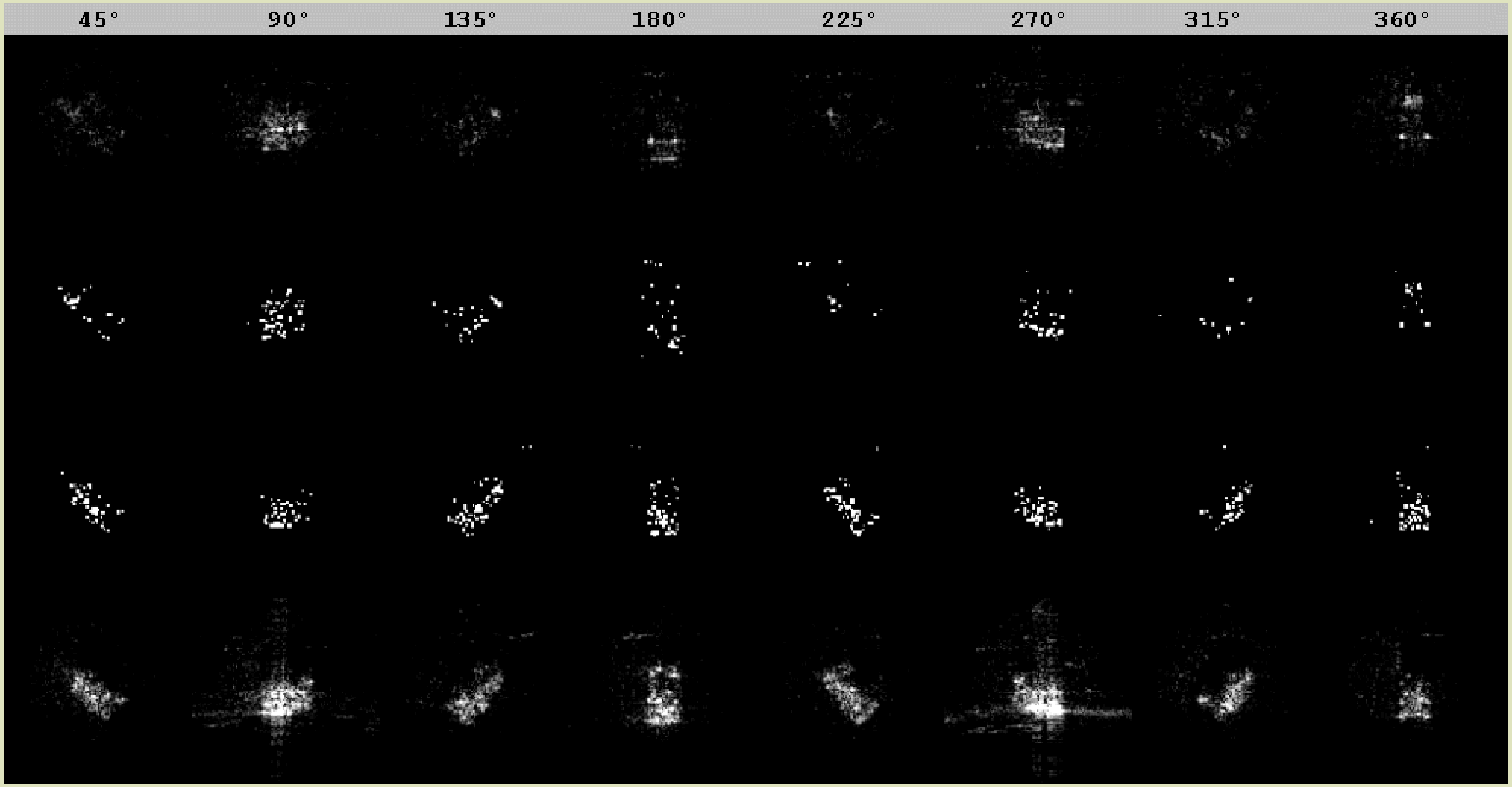

RCS image

Template

Template

RCS image

• Low RCS

• Less exctracted scatterers

Deception by decoy

Experiment F, evaluation

Classifier outcome:

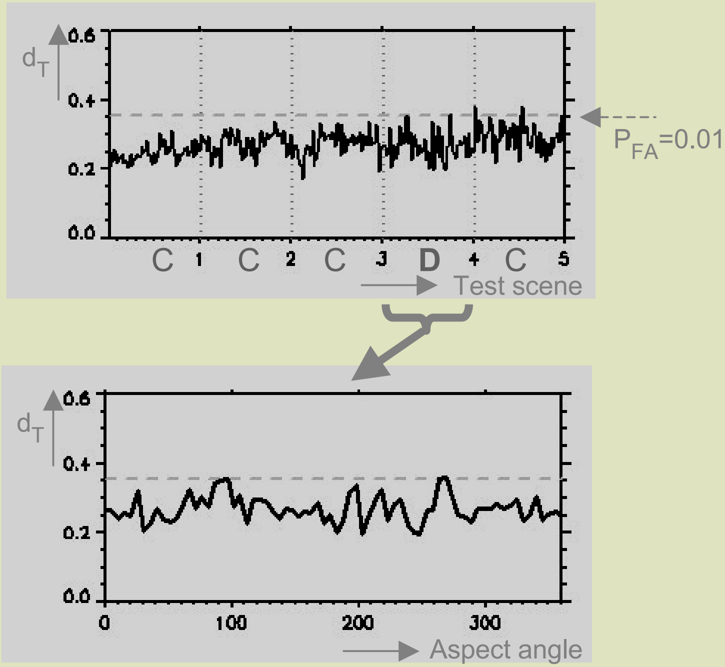

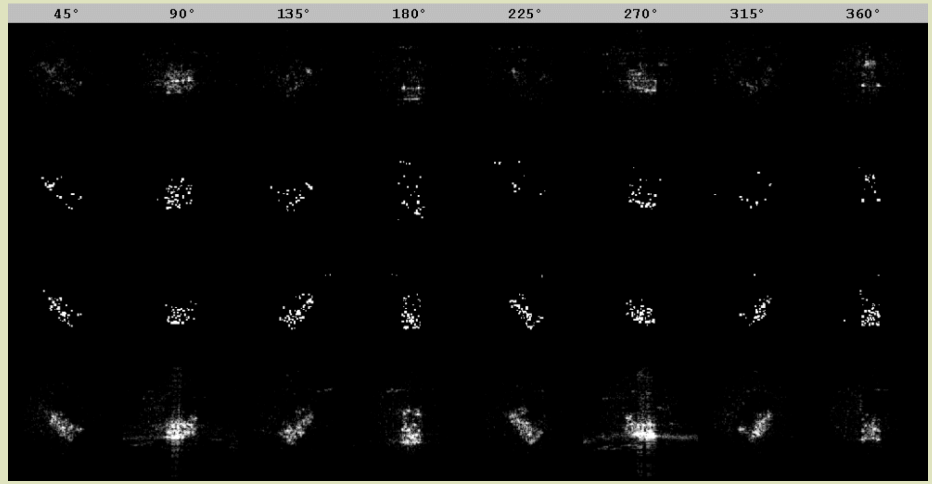

ROC curve, complete scene

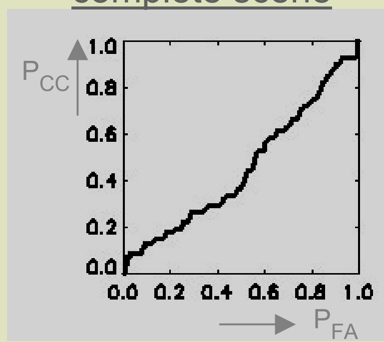

- No deception of the applied ATR system

Conclusions

- Effect on HR radar ATR performance mainly depending on degree of occlusion.
- Even with birch branches the ATR performance can be affected.
- Relative robustness of the ATR system, if only partially coverage with radar signal attenuating materials is applied.
- Impact on the ATR performance also possible by multi-path effects with a reflecting ground.
  - Test on concrete to be taken
- No deception by a decoy, designed for optical, infra-red sensors.
  - Test on radar decoy to be taken

Thank you for your attention!